

CHAPTER 1

Opportunities and Challenges for Transition Metal Catalysis in the Development of Materials for Deep Ultraviolet Lithography

Opportunities and Challenges for Transition Metal Catalysis in the Development of Materials for Deep Ultraviolet Lithography

Introduction and Historical Perspective

The last quarter of the 20th Century saw the rapid development and wide availability of powerful and reasonably priced microelectronics revolutionize nearly every aspect of our society from communications and science to shopping and entertainment. This rapid increase in affordable microprocessor power is directly attributable to the ability of the semiconductor industry to double the number of integrated circuit elements on the microprocessor roughly every 18 months, as described by Moore's Law.¹ This progress is driven by the associated cost advantages of producing more chips per wafer (2x more chips per wafer, 0.5x cost per chip). Advances in the science and engineering of lithography are critical to the continuation of this process.² At the forefront of these advances is the development of new imaging materials.

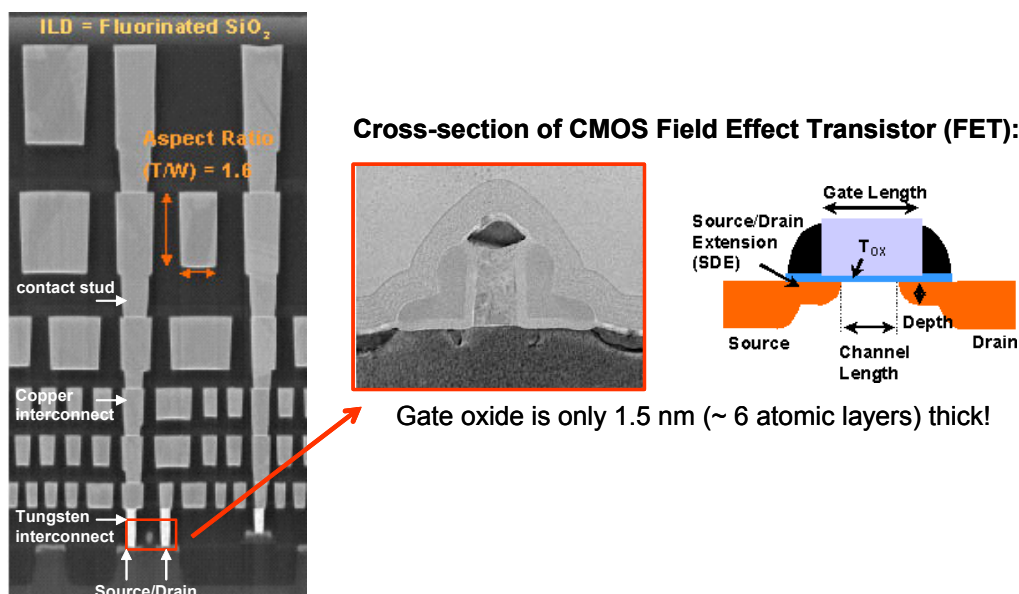


Figure 1.1. Cross-section of Intel Pentium[®] 4 (0.130 μm architecture)³

A cross-section of a commercially available computer chip (Intel Pentium® 4) based on 130 nm technology is shown in Figure 1.1.³ The Pentium® 4 features 77 million transistors, 60 nm gate lengths, and 6 layers of copper interconnects. These complicated structures are built up layer-by-layer through a several hundred step production process that involves many iterations of lithography. While the pitch of the interconnects (1.2 mm at the top level, 350 nm at the first metal level) can be achieved using older generations of lithography, the wafer-level features require the highest level of resolution and the latest generation of lithography.

At the time the work presented in this thesis began (early 2000), 248 nm lithography was the current state of the art production lithographic technique, 193 nm lithography was moving into optimization and process evaluation, and early research into 157 nm lithography and related imaging materials had just begun. In 1999, the International Technology Roadmap for Semiconductors (ITRS)⁴ put forth by the *International SEMATECH* detailed the timeline for possible lithographic solutions as shown in Table 1.1.

Table 1.1. 1999 ITRS Roadmap⁴

Year	1999	2002	2005	2008	2011
Feature Size	180 nm	130 nm	100 nm	70 nm	50 nm
Exposure Wavelength	248 nm	248 nm/193 nm	193 nm/ 157 nm	157nm /NGL	NGL
Radiation Source/Laser	KrF	KrF/ArF	ArF/ F₂	F₂ /EUV/EPL	EUV/EPL

While resist materials for 248 nm lithography had taken roughly 20 years to progress from initial discovery to final production quality performance and 193 nm resists had been under development for roughly 10 years, only five years remained for resist development before 157 nm lithography was expected to be introduced. The focus of this work as part of the *International SEMATECH* Universities Research Project (LITJ 102) was the development of advanced resist materials for 157 nm lithography. Although 157 nm lithography is no longer the lead candidate

to succeed 193 nm lithography as this is being written (late 2004) due to the rise to prominence of 193 nm immersion lithography,⁵ the lessons learned in this pursuit have not been in vain. Many of the material advancements achieved in the quest for 157 nm resist materials are currently being applied to the development of advanced resist materials for 193 nm immersion and next generation lithographies (NGLs) and are being back-integrated into production 193 nm resists. If 157 nm lithography resurfaces as an immersion technique in the future, many of the developments described in this work will be directly applicable.^{5a,e}

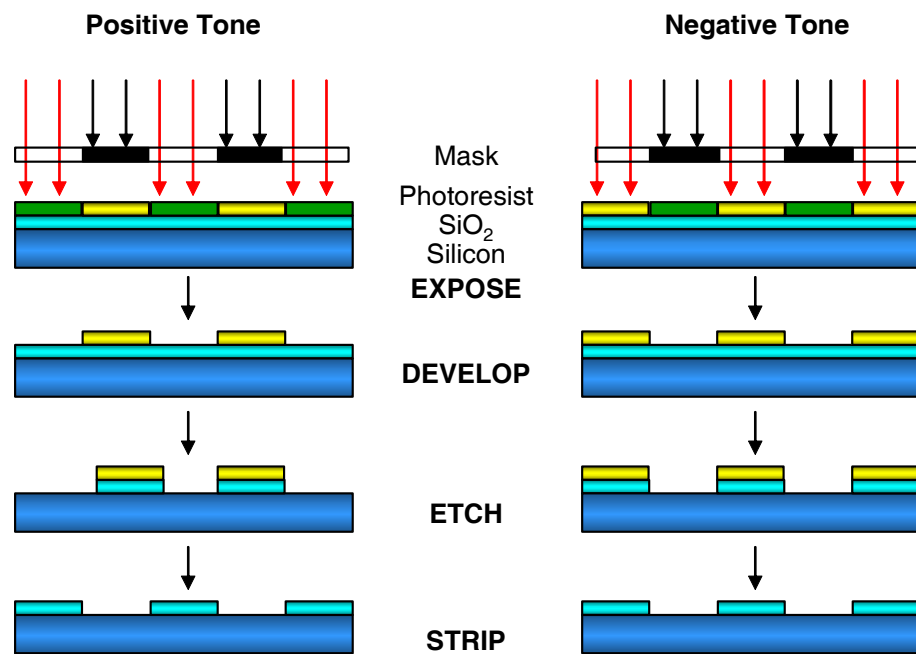


Figure 1.2. Photolithographic process

Introduction to Photoresists and Photolithography

Before the development of 157 nm resist material can be discussed, it is useful to review a brief description of photoresists and photolithography in order to understand the valuable resist design lessons learned during development of previous generations of lithographic materials. Optical lithography uses light to generate a pattern in a photosensitive polymer (photoresist) with subsequent transfer of that pattern onto the underlying substrate, as shown in Figure 1.2.² First, a

layer of photoresist is deposited onto a substrate via spin casting from a suitable solvent. Pattern formation is induced via illumination by a high-power laser light source through a complex series of optics involving a photomask. The interaction of the irradiating photons with the photosensitive elements in the photoresist leads to changes in the physical or chemical properties of the photoresist such as solubility, thermo-oxidative stability, molecular weight, etc. A dramatic change in solubility is the most commonly used approach, allowing the polymer in either the exposed (positive resist) or in the unexposed (negative resist) region to be washed away with an appropriate developing solvent. With the remaining photoresist acting as a protective layer, processes such as reactive ion etching (RIE) can be performed. Stripping of the remaining photoresist enables other post-lithography processes such as doping or dielectric deposition to be performed. In this fashion, IC devices are built layer-by-layer.

Ultimately, advances in lithography are governed by the physics of the optics. The resolution or feature size is governed by the “lens equation”

$$\text{Critical Dimension (resolution)} = k_1 \frac{\lambda}{\text{NA}},$$

k_1 is a process factor, λ is the wavelength of the light, and NA is the numerical aperture of the optics.² Unfortunately, the use of high power reduction optics (high numerical aperture) to minimize feature size results in a loss in depth of focus²

$$\text{Depth of Focus} \propto \frac{\lambda}{\text{NA}^2}.$$

Eventually, after optimization of exposure optics and process parameters, a shift to a shorter wavelength of light is required to achieve further reductions in feature sizes.

Photoresist Systems Photoresist systems are a complex mixture of matrix polymers, dissolution inhibitors, photoacid or photobase generators, buffers, and other additives.^{2,6} Hereafter, the matrix polymers will be referred to as photoresists, although these polymers by themselves may not be photoactive. Positive tone photoresist polymers generally consist of units

selected to offer etch resistance, adhesion to the substrate of interest, and some form of solubility switch as shown in Figure 1.3.⁷

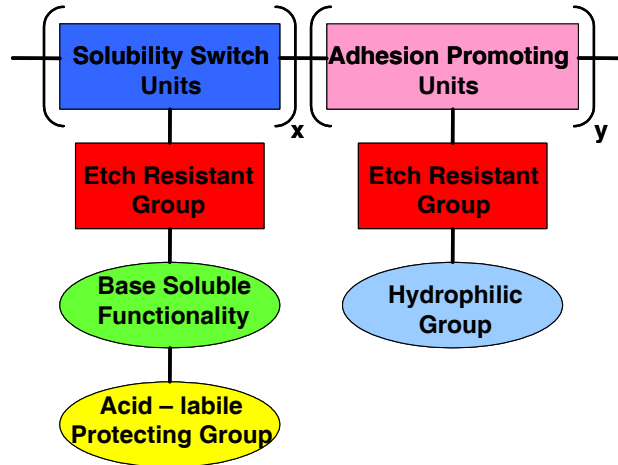


Figure 1.3. Design of a positive tone photoresist

Process	Required Photoresist Properties
Spin Casting	Solubility in suitable casting solvents Reasonable viscosity Good adhesion to wafer surface Phase compatibility with additives, photoacid generators...etc.
Post-application Bake	Thermal stability above T_g and b.p. of casting solvent
Exposure	Low absorbance at wavelength of irradiation ($\alpha_{10} < 0.7 \mu\text{m}^{-1}$) High sensitivity of photoactive species Minimal outgassing of volatiles
Post -exposure Bake	Thermal stability above T_g to allow acid diffusion ($T_g > 120 \text{ }^\circ\text{C}$) Rapid chemical reactions (low activation energies) ($< 60 \text{ s}$, $120 - 140 \text{ }^\circ\text{C}$) Minimal side reactions
Development	High contrast Good solubility in developer (0.262 N tetramethylammonium hydroxide) Rapid dissolution Low line edge roughness ($M_n < 10,000 \text{ Da}$) Good mechanical properties to resist pattern collapse
Etching	Good etch resistance - Similar to APEX (High carbon/hydrogen ratio) - Ohnishi parater < 3 (Low structural oxygen content)
General Considerations	Synthesis via simple, rapid, inexpensive, tolerant polymerization Low residual metal contamination ($< 20 \text{ ppb}$) Inexpensive, readily available, non-toxic materials

Figure 1.4. Material property requirements of a positive tone photoresist

The design of photoresist polymers is controlled by the large number of property requirements, some of which are outlined in Figure 1.4.⁶ Selection of appropriate structures to fill the roles described in Figure 1.3 involves a complicated balance of trade-offs. For example, the etch rate of a polymer has been empirically modeled by Ohnishi *et al.* as

$$\text{Etch Rate} \propto \frac{N_{\text{atoms}}}{N_{\text{carbons}} - N_{\text{oxygens}}}$$

where N_{atoms} , N_{carbons} , and N_{oxygens} are the numbers of atoms, carbons, and oxygens, respectively, in a repeat unit.⁸ Etch resistance is enhanced by increasing the relative carbon content of the polymer; however, most hydrophilic and base-soluble groups contain large amounts of structural oxygen which decreases etch resistance.

Chemically Amplified Photoresists for 248 nm Lithography For years, above wavelength imaging had been accomplished using diazonaphthoquinone-based novolac resists.^{2,6} Upon exposure to light, the diazonaphthoquinone is transformed via a Wolff rearrangement to an indene carboxylic acid. While the novolac matrix resin is insoluble in aqueous base in the presence of the diazonaphthoquinone, it becomes highly soluble in the presence of the carboxylic acid. Unfortunately, this dissolution inhibition approach does not possess high enough quantum efficiency for use with the less powerful laser light sources used in deep ultraviolet (≤ 248 nm) lithography.

In order to increase the quantum efficiency of the solubility switching reactions, a catalytic deprotection route was developed by Ito and Willson (Figure 1.5).⁹ This “chemically amplified” technique relies on the ability of a single photogenerated acid to deprotect as many as 100-200 latent base-soluble groups in a few seconds during a post-exposure bake. The most successful 248 nm photoresists are based on protected polyhydroxystyrene (PHOST) or N-blocked maleimide/styrene copolymers and feature large amounts of aromatic structures for high etch resistance (Figure 1.6).^{2,6,9} However, early chemically amplified resists showed extreme sensitivity to trace (< ppm) quantities of basic atmospheric compounds (primarily amine-based

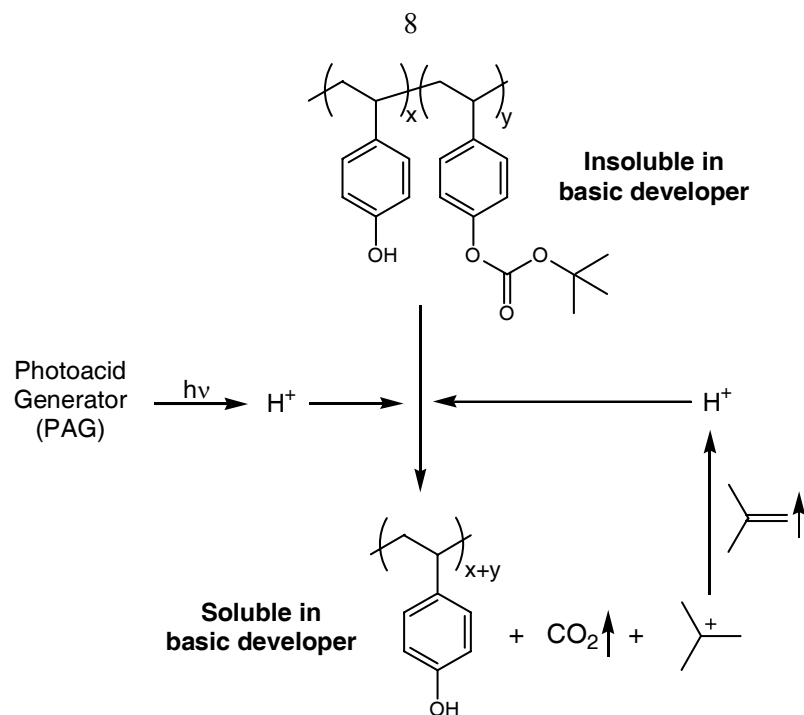


Figure 1.5. Chemical amplification

solvents used in paint and building materials). These airborne contaminants can penetrate the surface of the resist on the exposed wafer and quench the photogenerated acid, resulting in the production of an insoluble scum layer on the surface (T-topping). Environmentally stable, chemically amplified (ESCAP) resists were developed which incorporate a comonomer (such as *t*-butyl acrylate) which lowers the glass transition temperature (T_g) of the polymer below the

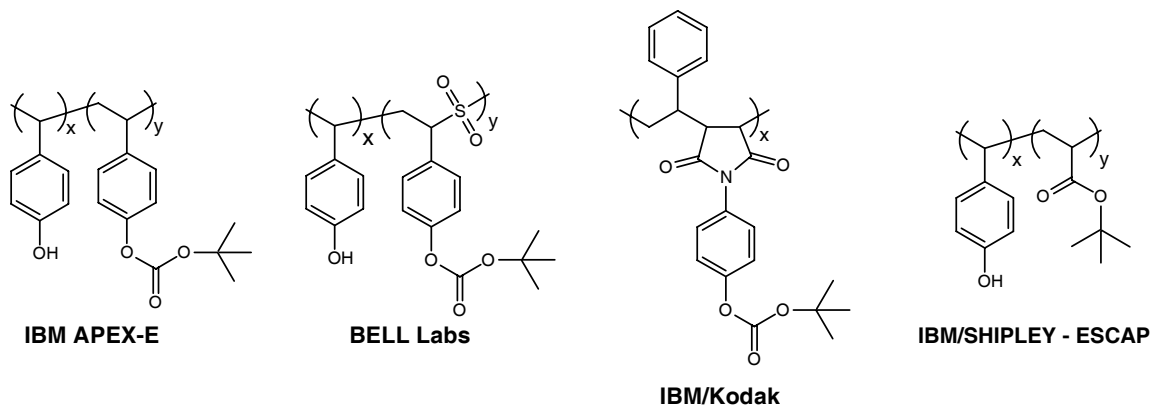


Figure 1.6. Commercially available 248 nm photoresists

thermal deprotection temperature.⁹ Annealing the resists above their T_g results in reduction of free-volume which decreases the rate of sorption and diffusion of atmospheric contaminants.

Remarkably, these resist materials experience a very large solubility change over a relatively narrow range of deprotection (Figure 1.7). Consequently, the ability of a small number of deprotection reactions to induce a step-like large solubility change is responsible for the high sensitivity and high contrast of chemically amplified resists. Namely, it allows these materials to efficiently produce step-type profiles rather than simply mirror the sinusoidal optical intensity profiles experienced during exposure.

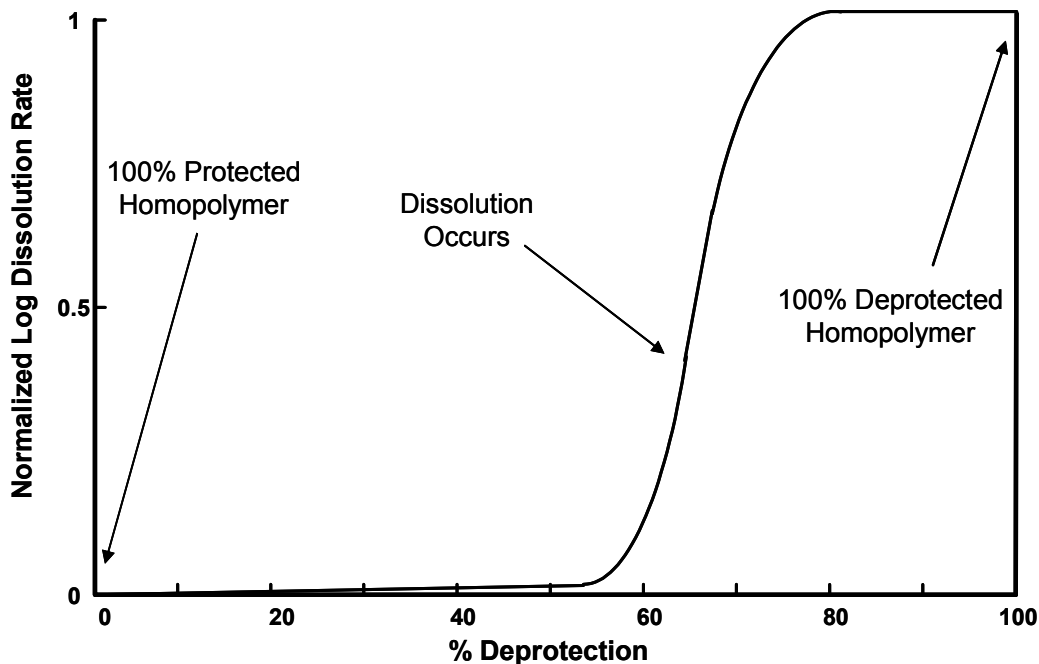


Figure 1.7. Dissolution rate as a function of deprotection for a model photoresist

193 nm Photoresists Unfortunately, the aromatic groups used to impart high etch resistance to 248 nm resists absorb too heavily for them to be useful at 193 nm.¹⁰ With heavily absorbing materials, the light intensity falls quickly as a function of depth into the material, resulting in muted features rather than the sharp, step-type profiles required. Fortunately, carbon-rich alicyclic structures were found to serve as suitable etch-resistant replacements for the highly

absorbing aromatic structures used in previous generations of lithography.¹⁰ A number of 193 nm resist platforms are under commercial development (Figure 1.8). Highly transparent acrylate and methacrylate polymers have been functionalized with alicyclic pendant groups (i.e., adamantyl and tricyclodecyl) to impart greater etch resistance to the oxygen-rich backbone.¹¹ Alternatively, functionalized norbornenes and tetracyclododecenes have been copolymerized with maleic anhydride via free radical techniques.¹² The anhydride group provides for excellent adhesion and serves as a latent water solubilizing group. Another leading class of commercial 193 nm photoresists in development is based on hybrid poly(methacrylate)-*co*-(norbornene-*alt*-maleic anhydride) copolymers.¹⁰

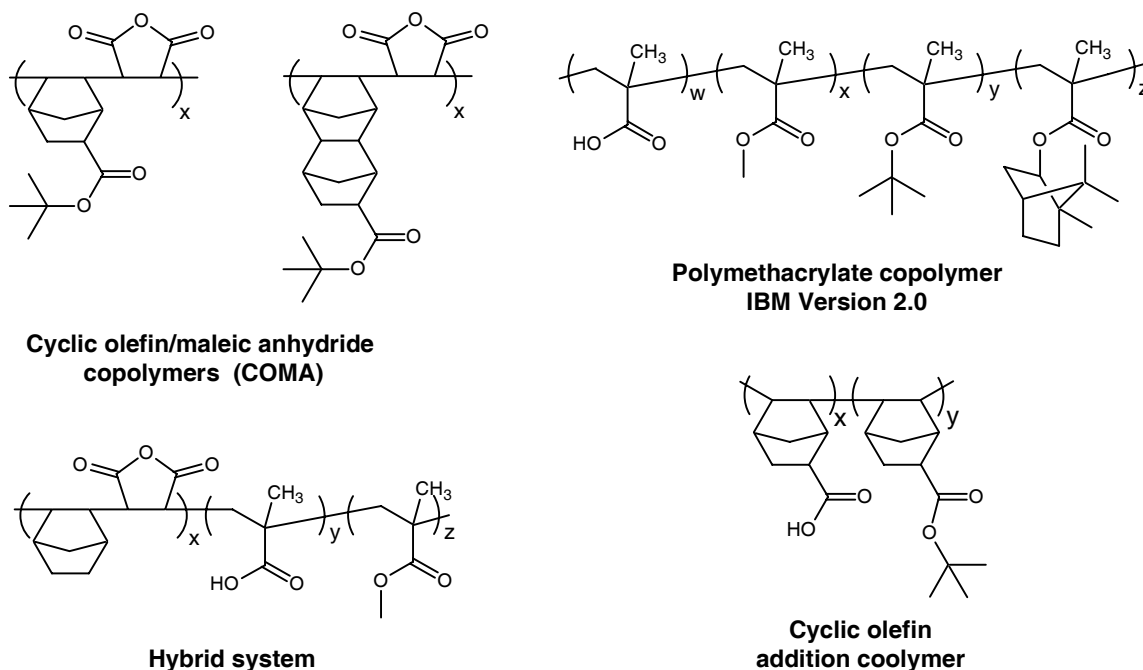


Figure 1.8. 193 nm photoresist polymers under development

Other groups have investigated metal-catalyzed polymerization of alicyclic monomers such as functionalized norbornenes and tetracyclododecenes.¹³ Unable to radically homopolymerize efficiently,¹⁴ norbornene-type monomers can be polymerized by transition metal catalysts to produce ring-opening metathesis (ROMP) or addition polymers. While a significant

amount of effort was expended exploring these polymers, the prospect of residual metal contamination has reduced the overall attractiveness of these materials.¹⁰

157 nm Materials Development

157 nm vacuum-ultraviolet (VUV) lithography initially appeared to be the most likely candidate for production of 100 nm structures around 2005.⁴ The ability to continue to utilize the tremendous amount of physical and intellectual capital invested in optical lithography was a reassuring prospect relative to the more risky option of adopting entirely new (and extremely expensive) next generation lithography (NGL) techniques such as extreme ultraviolet (13 nm, EUV), x-ray, and projection e-beam (SCALPEL, PREVAIL) lithography. While the development of a suitable illumination source (F₂ excimer laser, 157.6 nm) was achieved early on, it was the development and availability of the calcium fluoride optics which ultimately proved to be the stumbling block towards implementation.¹⁵

Early on, it appeared the chief optical problems were readily solvable; however, since O₂, water, and most polymers absorb heavily at 157 nm,^{16,17} the development of high transparency photoresists was considered to be the primary challenge facing 157 nm photolithography. Since carbon 2p ground state electrons are primarily responsible for absorption at 157 nm, carbon-carbon double bonds (olefins, aromatics), carbon-oxygen double bonds (aldehydes, ketones, esters), and even to some extent, carbon-hydrogen single bonds (hydrocarbons) are all unsuitable for use in 157 nm photoresists.¹⁶

These results are reflected in the measured absorption coefficients of a variety of common polymers and photoresists shown in Table 1.2.¹⁶ Due to their high absorbance at 157 nm, the use of the traditional photoresists used for 248 nm and 193 nm would require extremely thin films (30 - 50 nm) which would result in unacceptable levels of pinhole defects. In order for practical resist thicknesses (> 250 nm) to be employed, resist materials with an absorption coefficient less than 0.70 μm^{-1} is required. Silsesquioxanes and fluorocarbons are two classes of

Table 1.2. Necessary film thicknesses of common polymers and photoresists

Polymer	α_{10} [μm^{-1}]	Resist Thickness (optical density = 0.185) [nm]
Poly(hydrosilsesquioxane)	0.06 ^a	3083
Perfluoropolymer	0.70 ^a	264
Poly(norbornene-co-tetrafluoroethylene) (1:1)	1.10 ^b	168
Poly(dimethylsiloxane)	1.61 ^a	115
Poly(methyl trifluoromethacrylate)	2.68 ^c	69
Poly(phenylsiloxane)	2.68 ^a	69
Poly(vinyl alcohol)	4.16 ^a	44
Poly(methyl methacrylate)	5.42 ^c	34
Poly(norbornene) (addition)	6.10 ^a	30
Polystyrene	6.20 ^a	30
Poly(p-hydroxystyrene)	6.25 ^a	30
Poly(norbornene) (ROMP)	6.80 ^a	27
Sumitomo PAR-101	6.84 ^c	27
Shipley UV6-2D	6.85 ^c	27
IBM V1.0 acrylic terpolymer	8.20 ^a	23
Poly(chlorostyrene)	10.15 ^a	18
Poly(acrylic acid)	11.00 ^a	16

^a Data from ref. 16. ^b Data from ref. 29b. ^c Data from ref. 24a.

structures initially appearing to have sufficient transparency at 157 nm. However, while silicon-oxygen bonds are transparent at 157 nm, silicon-carbon bonds are only moderately transparent, complicating the development of resist materials. Additionally, the extremely large photon energy of 157 nm (~182 kcal/mol) results in significant amounts of homolytic bond cleavage of relatively weak chemical bonds such as carbon-chlorine and carbon-bromine bonds.¹⁸

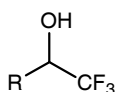
The ability of moderate amounts of fluorine to greatly increase 157 nm transparency combined with the high stability of the carbon-fluorine bond led most research labs to initially explore hydrofluorocarbon materials for 157 nm resists. While synthesis of fluorinated polymers is not trivial in itself, synthesis of a heavily fluorinated photoresist capable of dissolving in an aqueous base developer is an even more daunting challenge. Since all common polar groups used for solubility switching (*t*-butyl esters, *t*-boc, etc.) and adhesion (carboxylic anhydrides, alcohols, carboxylic acids) in traditional photoresist are heavily absorbing at 157 nm, the development of a polar, base soluble functionality suitable for 157 nm was the most pressing priority. The

phenolics and carboxylic acids characteristic of 248 nm and 193 nm resists owe their acidity to the resonance stabilization of their conjugate bases; however, the π -bonds responsible for this stabilization are too absorbing for use at 157 nm. Alternatively, fluorinated alcohols exhibit enhanced acidities relative to non-fluorinated aliphatic alcohols due to the inductive stabilization of the conjugate base. As shown in Table 1.3, the presence of fluorine substituents is sufficient to afford a pKa comparable to the phenolic groups employed in 248 nm resists.¹⁹ Fortunately, hexafluorocarbonols such as hexafluoroisopropanol are also highly transparent at 157 nm (Figure 1.9).²⁰ This discovery was particularly promising since the use of hexafluoroisopropyl alcohol groups had been investigated for use in 248 nm and 193 nm resists.²¹

Table 1.3. Acidity of fluorinated alcohols¹⁹

	Acid	pKa
	Water	18.3
	R = H	14.5
	Phenol	11.8
	R = CF ₃	11.2
	Acetic acid	6.3
	Pentafluorophenol	6.0

In 60/40 vol% DMSO/H₂O, 25 °C
Ionic strength 0.30 M (KCl)



In a search for chemical species that exhibit high transparency, several groups have used high level time-dependent density functional theory (TD-DFT) calculations to simulate the absorbance of simple chemical compounds at 157 nm.^{22,23} However, an empirical correction of the calculated transition energies is required for good agreement with experimentally measured vacuum-UV (VUV) spectra.²² Nevertheless, early computational results indicated that the absorption of esters could be dramatically decreased thru the addition of fluorinated substituents. The incorporation of fluorinated groups on the alkoxy portion of the ester results in a blue-shifting of the absorption band, while the addition of fluorinated substituents alpha to the ester

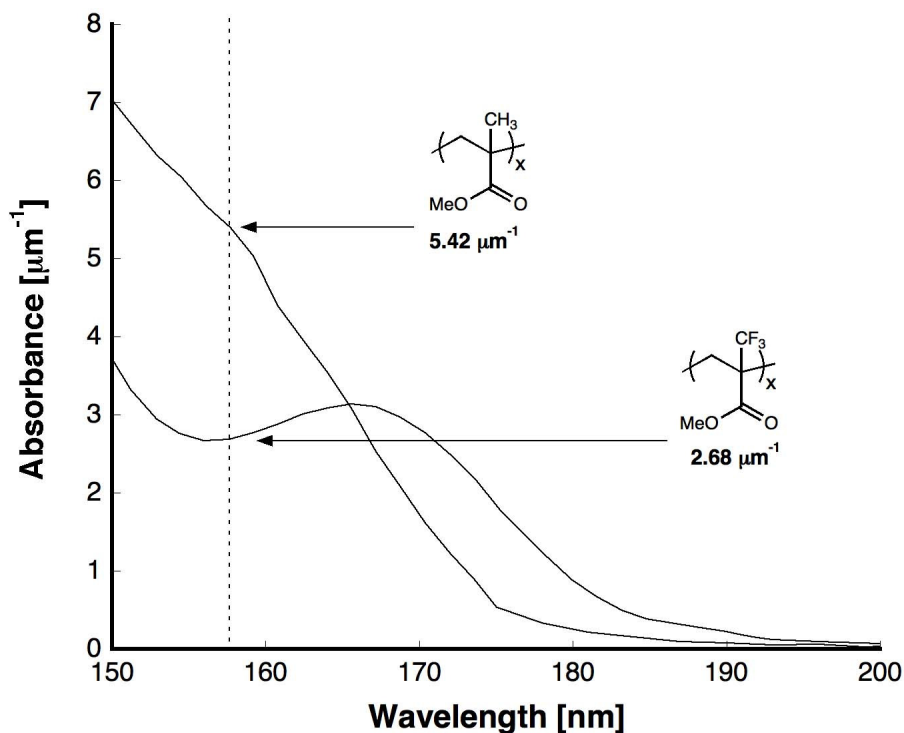


Figure 1.9. Effect of fluorination on transparency of polymethylmethacrylate²⁴

opens a window of transparency at 157 nm by red-shifting the absorption band.²² While a number of experimental VUV studies on model esters confirmed that ester transparency was increased with the incorporation of fluorinated substituents,²⁴ this is perhaps most dramatically illustrated by comparing the transparencies of poly(methyl methacrylate) and its fluorinated analogue²⁵ as measured by variable angle scanning ellipsometry (VASE)²⁶ (Figure 1.9).

With the discovery of a number of suitable polar groups, a number of photoresists based on fluorinated methacrylates,²⁷ fluorinated alcohols,²⁸ and hexafluorocarbonol-functionalized norbornene²⁹ were developed. However, the absorbance of these initial resist platforms, while being considerably more transparent than commercialized 248 nm and 193 nm resists, was still unacceptably high ($\sim 2\text{-}3.5 \mu\text{m}^{-1}$)^{24a} (Figure 1.10). The transparency of these 157 nm resists was a far cry from the transparency of successful 248 nm and 193 nm resists at their respective wavelengths as shown in Table 1.4.

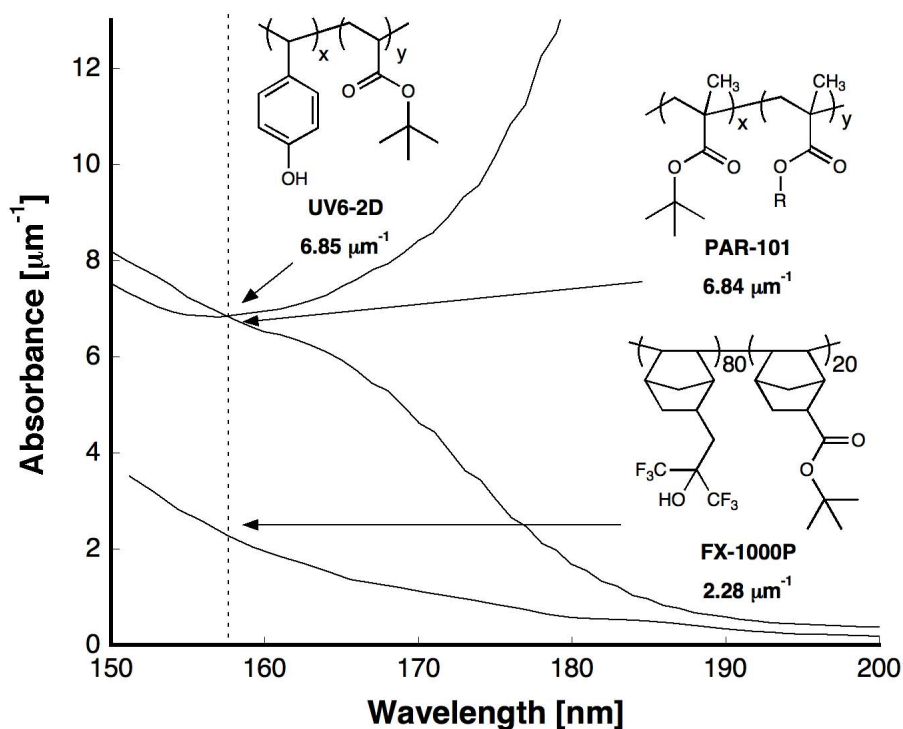


Figure 1.10. Comparison of initial 157 nm resist with previous generations (Structures shown for UV6-2D and PAR-101 only denote general class of resist)^{24a}

Table 1.4. Performance comparison of three generations of photoresists^{24a}

Resist	157 nm	193 nm	248 nm
UV6-2D (Shibley)	6.85	24.94	0.37
PAR-101 (Sumitomo)	6.84	0.47	0.06
FX-1000P (AZ-Clariant)	2.28	0.26	0.04

In order to increase the transparency of resist materials for 157 nm lithography, the incorporation of additional fluorine into the polymer backbone was required. Three distinct approaches emerged from the research community as shown in Figure 1.11. The metal-catalyzed norbornene addition polymer platform²⁹ was the first to be commercialized and offers high etch resistance (due to its purely alicyclic backbone), but suffers from relatively poor transparency. A series of radically polymerized aliphatic cyclopolymers³⁰ emerged which exhibit outstanding

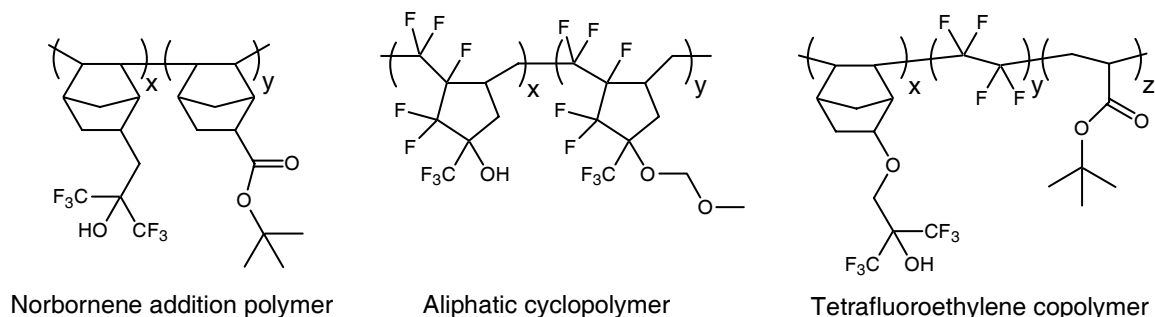


Figure 1.11. Three 157 nm photoresist platforms under development

transparency at 157nm ($\sim 0.5 - 0.7 \mu\text{m}^{-1}$); however, they offer lower resistance to etch processes. Free-radical copolymers of functionalized norbornenes with tetrafluoroethylene³¹ offer a good balance of transparency and etch resistance, while avoiding the issue of residual metal contamination.

Challenges and Opportunities for Metal Catalysis in Resist Development

While norbornene-type monomers do not undergo efficient radical homopolymerization, they can be copolymerized with electron deficient olefins such as maleic anhydride or tetrafluoroethylene to produce alternating copolymers described previously. Cationic polymerization of norbornenes is also inefficient and similarly results in polymers with 2,7-linkages rather than 2,3-linkages.¹⁴ Transition metal catalysis offers two routes to the efficient homopolymerization of norbornenes and functionalized norbornenes.¹³ Addition polymerization affords polynorbornenes with high glass transition temperatures ($> 300 \text{ }^\circ\text{C}$) due to the rigid backbone formed by 2,3-enchainment. Alternatively, ring-opening metathesis polymerization (ROMP) affords polymers with an unsaturated backbone and reduced glass transition temperatures. After hydrogenation, the ROMP polymers resemble the aliphatic cyclopolymer shown in Figure 1.11, but with 1,3-disubstitution of the cyclopentane structures rather than 1,2-disubstitution.

The focus of the work described in this dissertation is the improvement of the performance of metal-catalyzed addition and ring-opening metathesis polymers of norbornene via

the incorporation of additional fluorinated substituents and the resolution of the metal-catalyzed polymerization issues associated with these modifications.

Metal-catalyzed Addition Polymerization

The presence of much polar functionality in resist materials requires a great deal of functional group tolerance by the metal catalyst. A large number of neutral nickel³² and cationic palladium^{33,34,35} catalysts have been developed for the addition polymerization of functionalized norbornenes, a few of which are shown in Figure 1.12. Cationic palladium catalysts such as the (π -allyl) palladium catalysts developed by Risse *et al.* have been heavily studied in the literature.³⁴ The mechanism of norbornene polymerization for this catalyst is shown in Figure 1.13.³⁶ The active catalyst is formed via anion exchange of the chloride for a less coordinating anionic ligand. Norbornene displaces solvent and binds to the catalyst from its exo-face prior to insertion into the allyl palladium bond. The resulting allyl group forms a chelated intermediate which is a stable resting state for the catalyst. The dissociation/displacement of this chelated group by another norbornene monomer and subsequent norbornene insertion appears to be the rate limiting initiation step.³⁶ Subsequent polymerization is extremely rapid, with complete

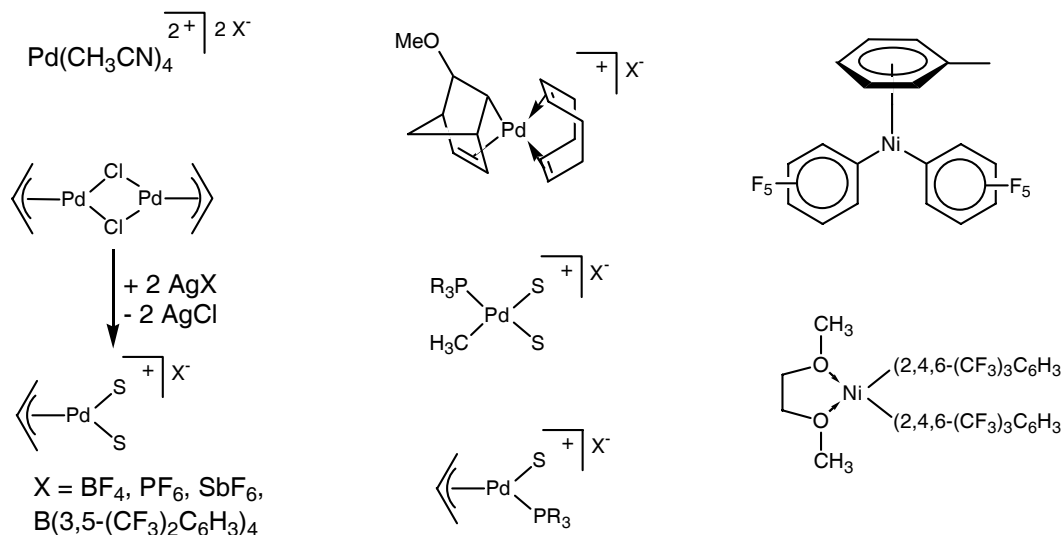


Figure 1.12. Common nickel and palladium addition catalysts

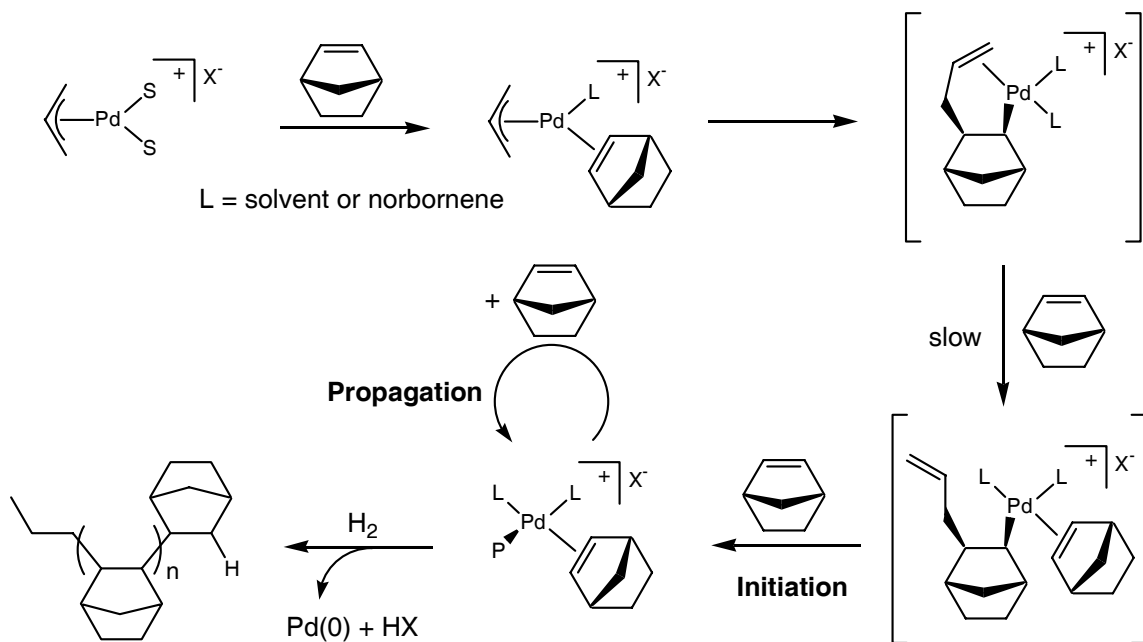


Figure 1.13. Mechanism of metal-catalyzed addition polymerization of norbornene

consumption of monomer within seconds. Polymerization of norbornene to high molecular weights is enabled by the absence of accessible β -hydrogens on the rigid alicyclic structure. The addition of small amounts of α -olefins provides for the β -hydrogens necessary for β -hydride elimination.³²⁻³³ This approach has been used to control the molecular weight of addition polymers; however, the resultant unstable palladium hydride often decomposes to palladium(0) rather than reinitiate another chain. Alternatively, dihydrogen can be used to remove the catalyst from the end of the polymer chain.

The presence of polar substituents on the norbornene typically results in a dramatic reduction in the rate of polymerization.³⁴ In addition, the rate of polymerization is highly dependent upon the *exo/endo* configuration of the substituent group on the norbornene, with *endo* isomers polymerizing significantly more slowly.³⁷ Unfortunately, the *endo* isomer is commonly the major product of the Diels-Alder synthesis of functionalized norbornenes.³⁸ The large difference in the rates of polymerization between *exo*- and *endo-n*-butyl-2-norbornene has been attributed to the steric compression of the vinyl hydrogen with the *endo*-functionality as it is

rehybridized from sp^2 to sp^3 during insertion.³⁷ For functionalized norbornenes, the chelation of the catalyst by the polar functional group to the endo-face of the norbornene was speculated to be also responsible for the reduction in polymerization rate. Geminally disubstituted norbornenes like the one shown in Figure 1.14 polymerize ~10 times slower despite the predominant exo-configuration of the ester group.³⁹ Subsequent work by Sen *et al.* has shown that the predominant rate decelerating interaction is the simple binding of the polar functional group to the cationic metal center.^{37b} As a result of their theoretical calculations, Ziegler *et al.* proposed that neutral catalysts offer potentially superior performance due to their reduced preference for polar functional groups while retaining similar ability as cationic metal centers to bind olefins.⁴⁰ Recently, Sen *et al.* confirmed this by demonstrating the ability of a neutral palladium catalyst to polymerize exo and endo isomers of functionalized norbornenes at more similar rates; however, these catalysts currently have insufficient activity to be useful.^{37a}

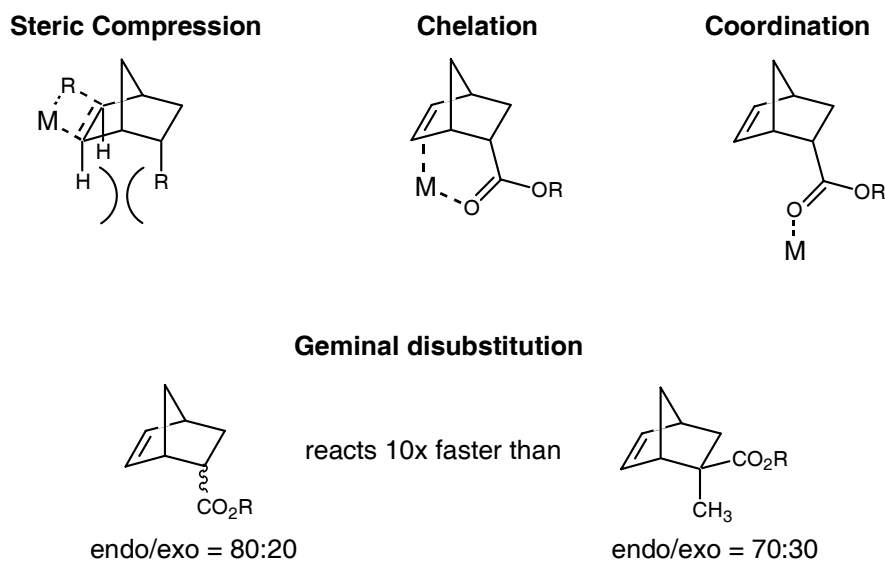


Figure 1.14. Issues in the polymerization of functionalized norbornenes

Design of Transparent Addition Polymers for 157 nm Photoresists

In order to design fluorinated norbornenes with higher transparencies, careful attention must be paid to the effects of fluorine on the polymerization activities of the resulting monomers. For example,

fluorinated olefins have insufficient electron density to bind to metal centers and undergo polymerization. A number of partially fluorinated norbornanes have been synthesized and examined by vacuum ultraviolet spectroscopy by Willson *et al.* (Figure 1.15).⁴¹ It can be seen that di-substitution is more effective at increasing transparency than mono-substitution, and substitution at the 2-position is more effective than substitution at the 7-position.

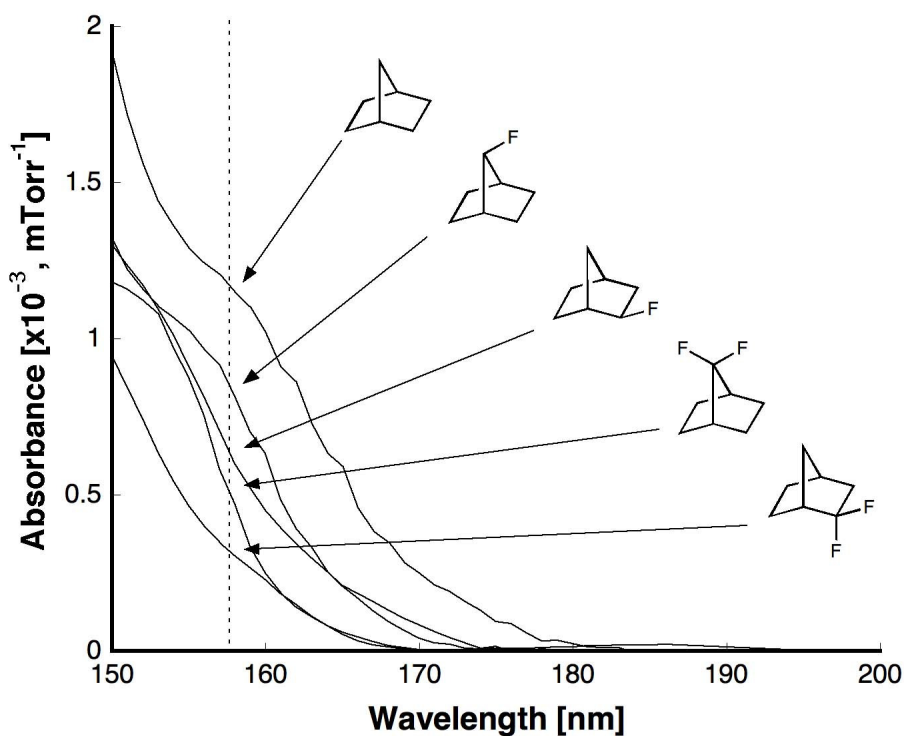


Figure 1.15. Effects of fluorination on norbornane transparency⁴¹

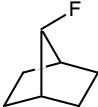
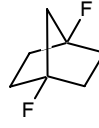
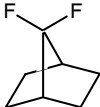
						
Itani <i>et al.</i> ^{42c}	100	-	-	30	14	12
Dixon <i>et al.</i> ^{42a/b}	100	61	52	52	29	25
Experimental ⁴¹	100	76	58	-	48	29

Figure 1.16. Relative calculated absorbances of fluorinated norbornanes

While theoretical calculations of the vacuum ultraviolet spectra of a number of fluorinated norbornanes qualitatively agree with the experimental observations,⁴² the calculated values tend to overestimate the relative transparency when compared to experimentally determined values, even with empirical corrections (Figure 1.16).

Alternatively, several other bicyclic olefin systems exist which have additional carbons where fluorinated substituents could be placed. Chief among these are bicyclo[2.2.2]oct-2-enes formed via the Diels-Alder reaction of 1,4-cyclohexadiene with electron deficient olefins. Unfortunately, bicyclo[2.2.2]oct-2-ene is unreactive towards metal-catalyzed addition polymerization.⁴³ This lack of reactivity is illustrated by the relative rates of dipolar cycloaddition shown in Table 1.5.^{44,45} The low ring-strain of the [2.2.2] system (similar to that of cyclohexene) results in poor reactivity.⁴⁴ However, norbornene exhibits reactivities even greater

Table 1.5. Reactivities of cyclic and bicyclic olefins^{44,45}

	Strain Energy (kcal/mol)	Relative Strain Energy (to saturated compound) (kcal/mol)	Relative rate of Dipolar Cycloaddition*
	15.8	6.0	3000
	25.2	9.0	
	10.3-11.7	0.8-2.2	5
	1.4	1.5	1
	5.9	-0.3	
		10.0*	2300
		8.9*	2300

* 2,4,6-trimethyl benzonitrile oxide, CCl₄, 25 °C⁴⁴

than its ring strain would predict. The asymmetric distribution of the π -bond electron density from exo face of the olefin coupled with the low steric shielding of the exo face results in particularly high reactivity. Unlike norbornene, the methylene protons in bicyclo[2.2.2]oct-2-ene may also sterically hinder approach of a metal catalyst to the olefin. A few other highly strained bicyclic systems exist, but their synthesis is not trivial and unlikely to be successful on the scales required for application as photoresist materials. As a result, norbornene-type monomers are the only practical bicyclic olefins for use in resist material development.

Having determined the effect of fluorination on transparency, a second-generation addition polymer featuring was designed as shown in Figure 1.17. Since the absorbance of the ester-functionalized norbornane in the first-generation addition polymer is far greater than the more transparent hexafluorocarbonol-functionalized monomer, the effect of an additional trifluoromethyl group on the overall absorbance of the copolymer was expected to be dramatic.

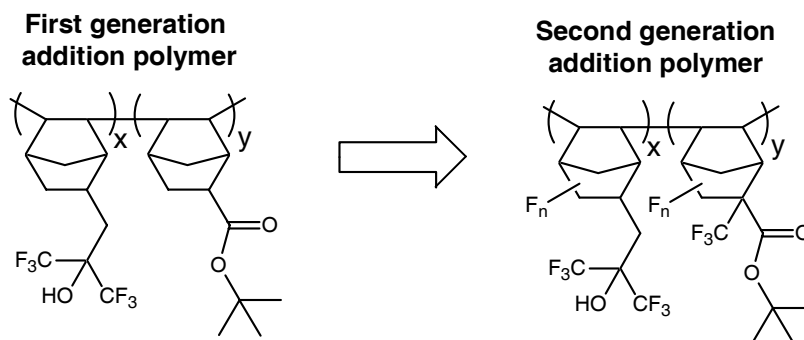


Figure 1.17. Design of transparent addition polymers for 157 nm lithography

The synthesis of an ester-functionalized norbornene from the 2-trifluoromethyl-acrylate proceeded smoothly and the saturated analogue exhibited improved transparency at 157 nm as expected (Figure 1.18).²⁴ Unfortunately, this monomer was found to be unreactive towards metal-catalyzed addition polymerization with both nickel and palladium catalysts.²⁹ Only trace amounts were incorporated with copolymerizations with the hexafluorocarbonol-functionalized

norbornene. The two heavily electron-withdrawing substituent groups reduce the polymerization activity by reducing the electron density of the norbornene via induction. When this inductive deactivation is coupled with the additional order of magnitude lower reactivity of norbornenes with geminal substituents, the result is a monomer with virtually no polymerization activity.

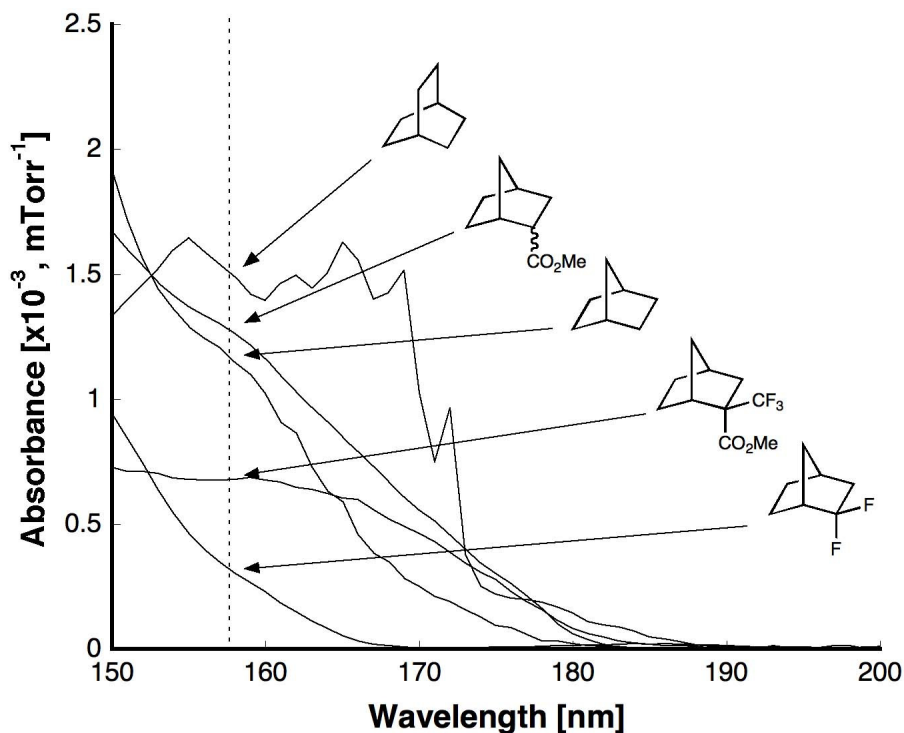
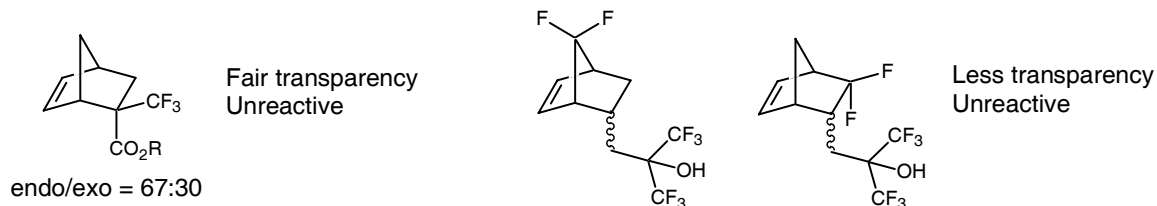


Figure 1.18. Transparency of fluorinated norbornanes for 157 nm photoresists²⁴
(Poor spectrum of bicyclo[2.2.2]octane due to low volatility)

Synthesis of difluorinated versions of the hexafluorocarbonyl-functionalized norbornane resulted in similarly discouraging results (Figure 1.19).⁴⁶ First, the structures exhibited *increased* absorbance relative to the base monomer. Secondly, the more fluorinated monomers were found to be unreactive towards metal-catalyzed addition polymerization. The larger fluorine substituent in the 7-syn position may sterically block or interact with the approaching catalyst and thereby prevent polymerization. However, the detrimental impact of additional fluorine incorporation at the 2-position was surprising. These efforts to produce norbornene addition polymers with

193 nm Version**157 nm Version****Figure 1.19.** Detrimental effects of increased fluorination

enhanced transparency at 157 nm through the selective incorporation of additional fluorine are summarized in Figure 1.19. Two key lessons have been learned through these failures; geminal disubstitution must be avoided and the additional fluorine must be placed as far away from the reactive olefin as possible.

We hypothesized that the incorporation of additional cyclic units on the norbornene could provide a scaffold for additional fluorinated substituents while reducing the steric and electron interference with the subsequent polymerization. Chapters 2 and 3 of this thesis detail the synthesis and polymerization of new fluorinated tricyclo[4.2.1.0^{2,5}]non-7-enes, respectively. Similarly, chapters 4 and 5 describe the synthesis and polymerization of two new classes of alicyclic olefins, 3-oxa-tricyclo[4.2.1.0^{2,5}]non-7-enes and 4-oxa-tricyclo[4.3.0^{1,6}.0^{3,7}]non-8-enes. Finally, the synthesis of new, transparent difunctional monomers containing both hexafluorocarbon and ester functionalities are described in Chapter 6. These new classes of monomers and materials illustrate potential highly transparent resist materials for 157 nm lithography.

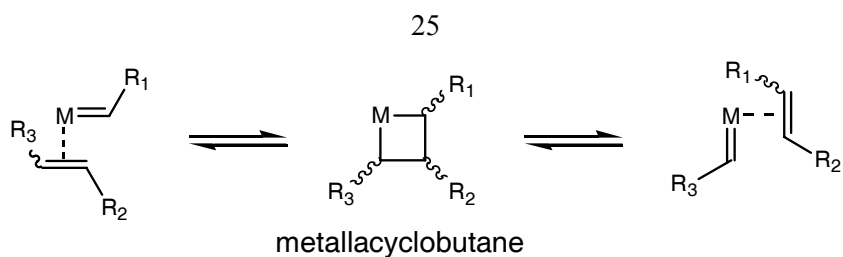


Figure 1.20. Olefin metathesis

Ruthenium-catalyzed Olefin Metathesis

Olefin metathesis involves the metal-carbene mediated cleavage and recombination of carbon-carbon double bonds as shown in Figure 1.20.⁴⁷ The process proceeds through the formation of a metallacyclobutane intermediate. When the reaction is used to α,ω -diene can undergo ring-closing metathesis (RCM)⁴⁹ to form a cyclic olefin if the resultant ring has low ring-strain (usually 5, 6, and 7-membered rings), as shown in Figure 1.21. Otherwise, the α,ω -diene may undergo acyclic diene metathesis (ADMET)⁵⁰ polymerization to form oligomeric and eventually polymeric materials in a step-growth process. However, the most facile route to polymeric material is the polymerization of strained cyclic olefins such as norbornene via chain-

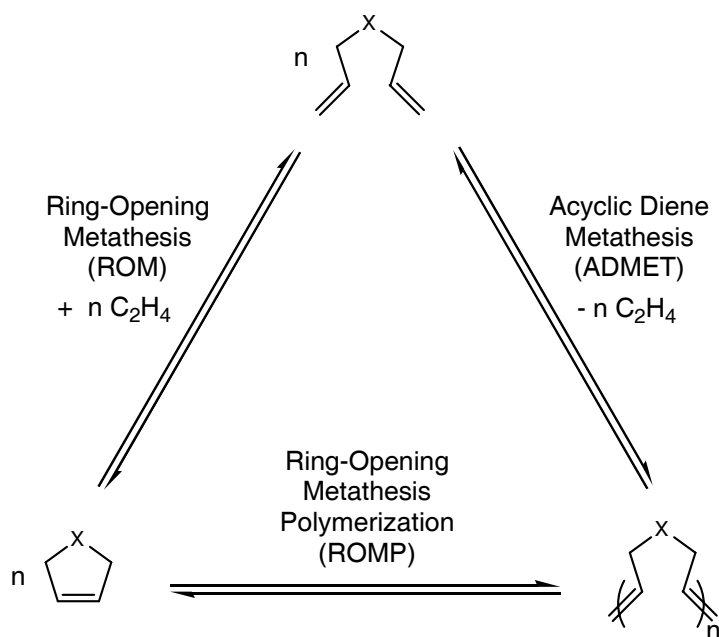


Figure 1.21. Olefin metathesis processes

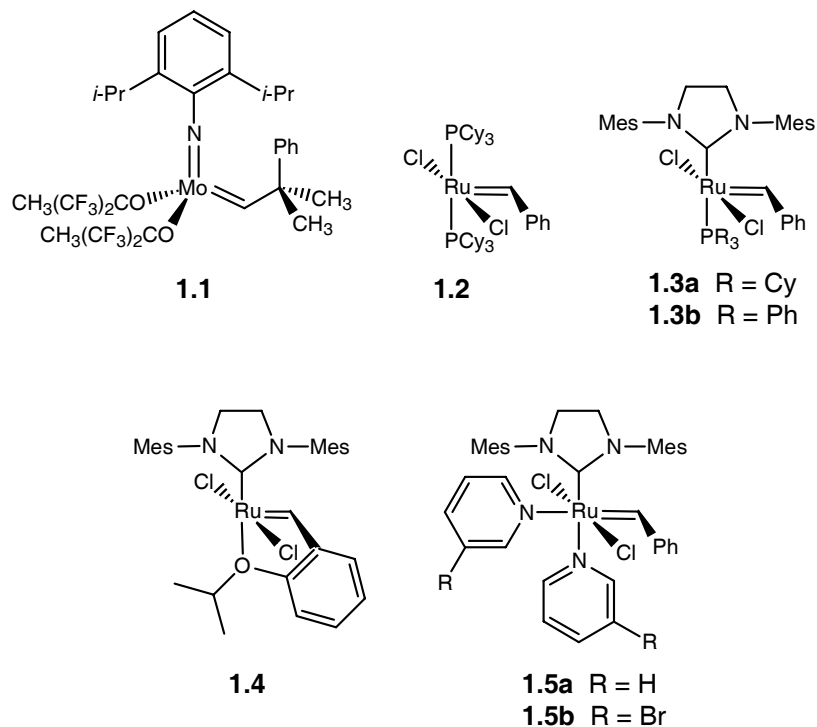


Figure 1.22. Olefin metathesis catalysts

growth ring-opening metathesis polymerization (ROMP).^{51,52}

The use of olefin metathesis has mirrored the development of well-defined metal carbene olefin metathesis catalysts such as catalyst **1.1** (Figure 1.22).⁵³ However, early transition metal molybdenum and tungsten catalysts have limited abilities to tolerate polar functional groups (such as alcohols, ketones, and esters) and require rigorous purification and drying of reagents and reaction solvents.⁵⁴ Fortunately, a renaissance in olefin metathesis has occurred over the last 8 years with the development of highly active, functional group tolerant olefin metathesis catalysts based on ruthenium such as **1.2**.⁵⁵ More recently, the use of strongly donating N-heterocyclic carbene ligands has resulted in the recovery of the activity loss once associated with the move to a late transition metal and afforded catalysts such as **1.3** with higher activities, stabilities, and functional group tolerances.^{53,56} In further optimization of the ligand set, phosphine-free systems with enhanced stability or initiation rates have been developed (catalysts **1.4** and **1.5**, respectively).^{57,58} While **1.2** has been used to catalyze the controlled living polymerization of

functionalized norbornenes, the greater reactivity and much higher initiation rates of catalyst **1.5** allows the living polymerization of less reactive endo-substituted norbornenes and results in polymers with narrower polydispersities.⁵⁹

These recent developments in metathesis catalysts are particularly beneficial to the potential synthesis of highly functionalized photoresist polymers via ROMP. A particular benefit of ROMP is the facile control of molecular weight via chain transfer, a process that is not trivial in metal-catalyzed addition polymerizations. The ability to control molecular weight by chain transfer offers the ability to employ very low catalyst loadings. Polymer molecular weights may be controlled either kinetically or thermodynamically through the use of terminal or internal olefinic chain transfer agents (CTAs) (Figure 1.23).⁶⁰ The first generation, bisphosphine-based catalyst **1.2** cannot perform secondary metathesis reactions on the olefins in the polymeric backbone and is significantly more reactive towards terminal rather than 1,2-disubstituted olefins.

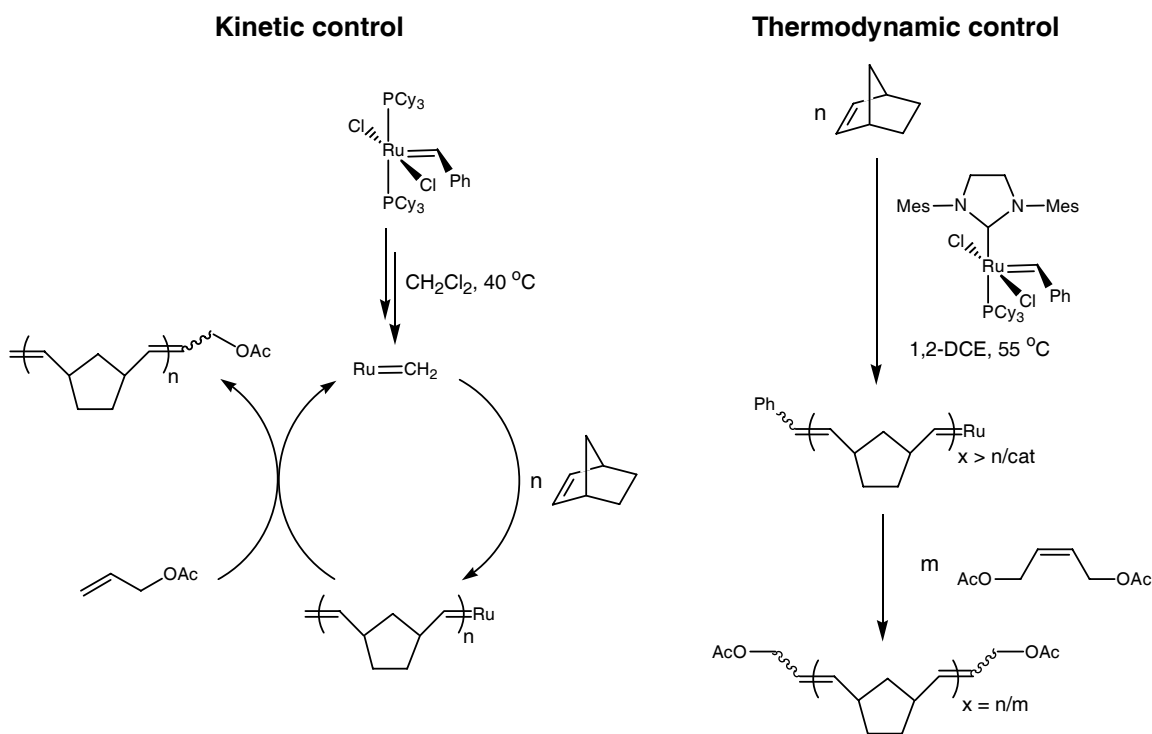


Figure 1.23. Control of molecular weight via chain transfer in ROMP

Therefore, the use of terminal olefin CTAs affords a kinetic control of the molecular weight that is dependent upon the monomer to chain transfer agent ratio $[M]/[CTA]$. The use of a functionalized CTA results in the formation of end-functionalized poly(norbornene)s.⁶⁰

Alternatively, the second generation catalyst **1.3** can perform secondary metathesis on the backbone olefins of poly(norbornene) at slightly higher temperatures. The slow initiation rate and fast propagation typically results in the formation of very high molecular weight material. Secondary metathesis reactions subsequently redistribute the end-groups introduced by the presence of a chain transfer agent to afford a molecular weight distribution that is determined by the monomer to chain transfer agent ratio $[M]/[CTA]$. The use of a symmetric chain transfer agent has been used to produce telechelic poly(norbornene)s.⁶⁰

Design of a ROMP-based 157nm Photoresist The major disadvantages of norbornene ROMP polymers are the residual double bonds which must be hydrogenated to afford the polymer with acceptable oxidative stability and the resulting low glass transition (T_g) temperatures. The glass transition temperature of norbornene ROMP polymers typically fall by around 30 °C after hydrogenation.⁶¹ A series of norbornene ROMP polymers and their glass transition temperatures are shown in Figure 1.24. It should be noted that the glass transition temperature of ROMP polymers is heavily influenced by the cis/trans ratios of the backbone olefins and the polymer tacticity, both of which are highly catalyst dependent. The examples shown in this chapter are taken from the literature and are not polymerized under identical conditions; therefore, the glass

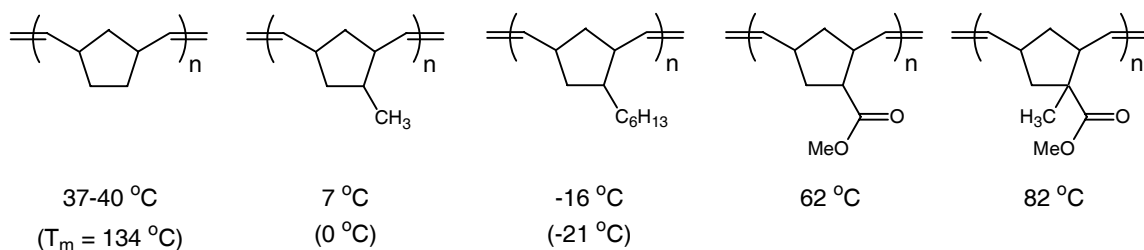


Figure 1.24. Glass transition temperatures of norbornene ROMP polymers⁶¹⁻⁶³
Values in parentheses are for the hydrogenated analogues

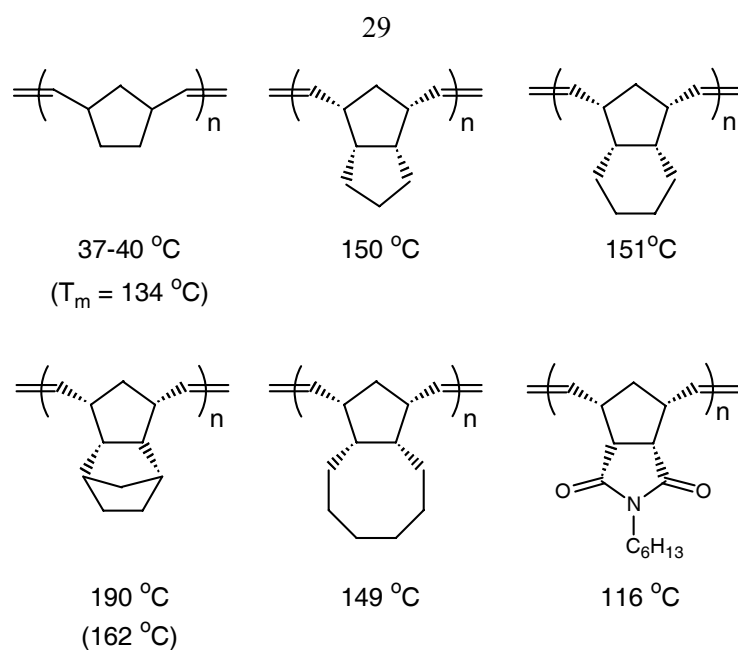


Figure 1.25. Effect of additional cyclic units on glass transition temperature^{61,63,64}
Values in parentheses are for the hydrogenated analogues.

transition temperatures cited here are only useful for a general comparison. The difference in T_g between the ROMP polymers shown here and norbornene addition polymers (> 300 °C) is dramatic.

In order to increase the glass transition temperature of ROMP polymers, additional cyclic structures are often incorporated; however, Stelzer *et al.* have shown that the T_g is relatively unaffected by the size of the additional cyclic structure (Figure 1.25).⁶⁴ Tetracyclo[4.4.0.1^{2,5}.1^{7,10}]dodec-3-enes (TCDs) are synthesized during the Diels-Alder synthesis of norbornenes via the addition of an extra cyclopentadiene unit. ROMP polymers of several TCDs have acceptable glass transition temperatures for use as photoresists. Incorporation of polar ester substituents can raise the glass transition temperature. However, additional steric bulk has a decreased effect on the T_g the further it is away from the backbone. For example, while the addition of a methyl group alpha to the ester raises the T_g of a polynorbornene by ~ 20 °C (Figure 1.24), it has virtually no effect on a TCD ROMP polymer (Figure 1.26). Extremely large groups such as the adamantyl group in the maleimide-functionalized poly(norbornene) are required to

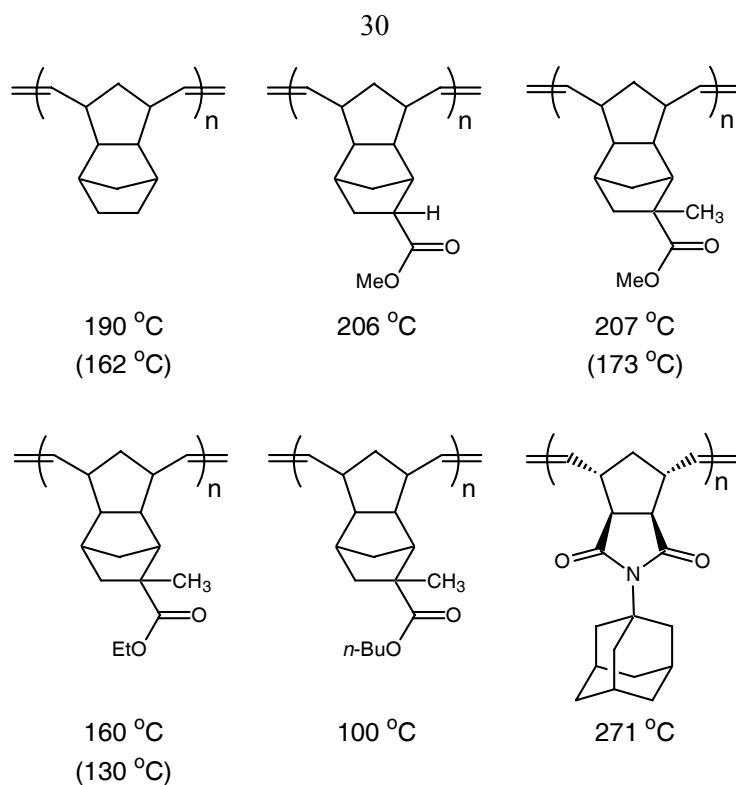


Figure 1.26. Effect of substituents on glass transition temperature^{61,63,65}
Values in parentheses are for the hydrogenated analogues.

boost the T_g above $250\text{ }^{\circ}\text{C}$.⁶⁵ In addition, the presence of long, flexible substituents counteracts the benefits of the extra cyclic structure and significantly reduces the polymer's T_g .

While the tricyclodecane backbone structure of a TCD ROMP polymer should have similar etch resistance to adamantane given its similar Ohnishi parameter,^{12e} theoretical calculations suggest that the tricyclodecane structure should have higher absorption at 157 nm than many other alicyclic structures (cyclopentane < norbornane < cyclohexanone = adamantane < tricyclodecane).⁴² In fact, tricyclodecane appeared to be about 3 times more absorbing than cyclopentane and around 0.33 times more absorbing than norbornane. These calculations suggest that an absorption penalty will be incurred by using additional cyclic units to boost T_g . The use of additional fluorine substituents will be necessary to offset this inherent disadvantage.

ROMP of fluorinated norbornenes and norbornene-type monomers has been explored with a wide variety of ill-defined and early transition metal catalysts.⁶⁶ A few examples of

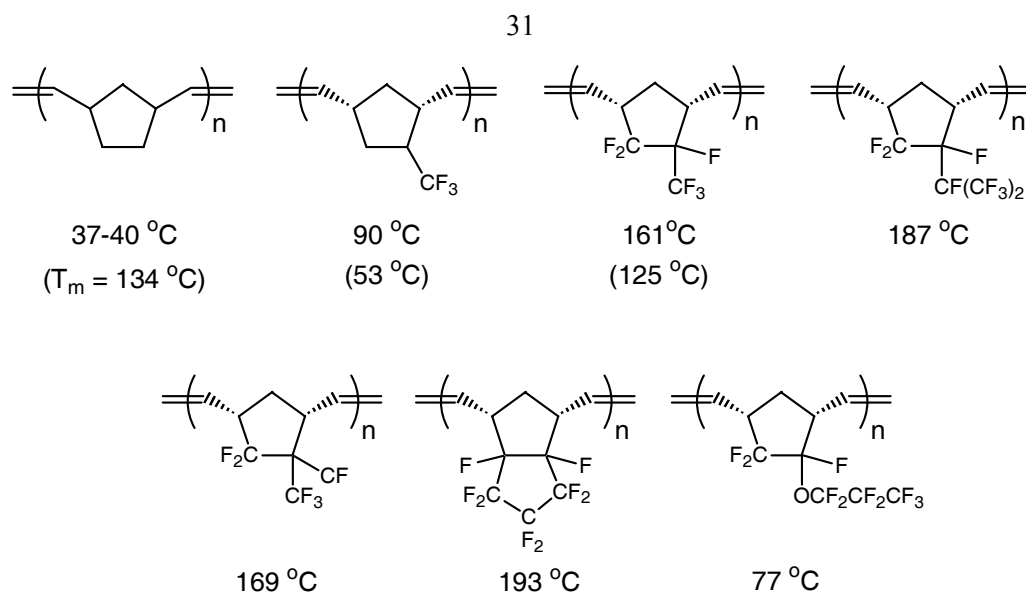


Figure 1.27. ROMP polymers of fluorinated norbornenes⁶⁵

ROMP polymers of fluorinated norbornenes that have been studied are shown in Figure 1.27. The activity of the newer second-generation ruthenium metathesis catalysts is likely high enough to polymerize these fluorinated norbornenes. While the glass transition temperatures of several of these monomers appear to be promising for use as 157 nm resist materials, the location of the fluorinated groups so close to the olefin raises the distinct possibility of reactivity ratio concerns when copolymerized with more electron-rich monomers. Unfortunately, these fluorinated ROMP polymers are reportedly difficult to hydrogenate fully (perhaps due to their unique solubilities).

Ring-opening metathesis polymers were briefly examined for use as 193 nm resists.¹³ A number of copolymers of functionalized norbornene and TCD monomers were synthesized using an ill-defined iridium catalyst. In order to achieve acceptable glass transition temperatures, the incorporation of a significant quantity of free carboxylic acid was required (Figure 28).⁶⁷ These polymers exhibited swelling problems, poor adhesion, slow dissolution, and phase incompatibility with several photoacid generators. In order to overcome this past poor performance, the use of more active, second generation ruthenium catalysts is expected to provide substantially better molecular weight control and lower residual metal content. The good

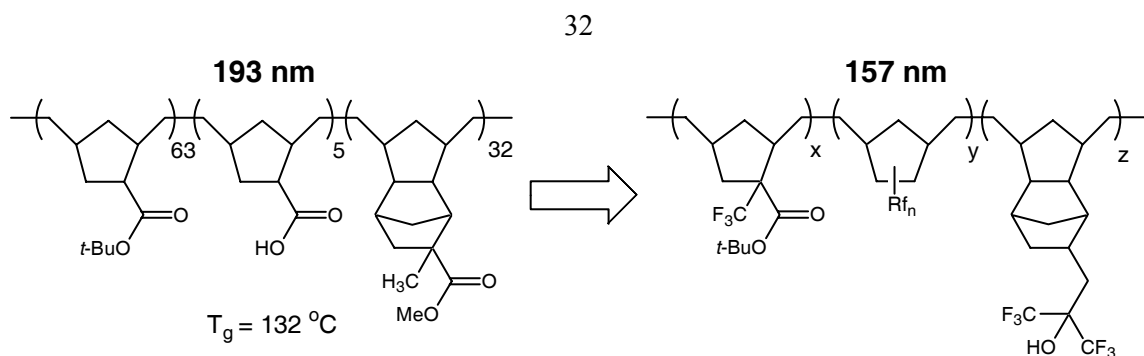


Figure 1.28. Design of ROMP-based resists for 157 nm lithography

dissolution behavior and adhesion properties of hexafluorocarinols are expected to overcome related problems with the 193 nm ROMP materials. An additional fluorinated norbornene-type monomer (possibly of the type shown in Figure 1.28) will be necessary in order to afford acceptable glass transition temperatures and to offset the potentially higher absorbance of the tricyclodecane structure. Chapter 5 of this thesis details the synthesis of a new class of transparent, fluorinated 4-oxa-tricyclo[4.3.0^{1,6}.0^{3,7}]non-8-ene monomers suitable for increasing the glass transition temperature of ROMP polymers. Finally, chapter 6 describes a few aspects of ROMP polymerization of the hexafluorocarinol-functionalized TCD monomer related to polymer transparency at 157 nm and the exploration of several other alicyclic structures for high T_g , metathesis-based materials.

References and Notes

- (1) (a). Moore, G. E. *Electronics* **1965**, 38, 114. (b). Moore, G. E. *Proc. SPIE* **1995**, 2439, 2.
- (2) (a). Walraff, G. M.; Hinsberg, W. D. *Chem. Rev.* **1999**, 99, 1801-1821. (b). Brunner, T. A. *J. Vac. Sci. Technol. B* **2003**, 21, 2632-2637.
- (3) Thompson, S.; Alavi, M.; Hussein, M.; Jacob, P.; Kenyon, C.; Moon, P.; Prince, M.; Sivakumar, S.; Tyagi, S., Jr.; Bohr, M. *Intel Technol. J.* **2002**, 6, 5-13. Graphs used by permission from Intel Corporation as published in Thompson, S.; Alavi, M.; Hussein, M.; Jacob, P.; Kenyon, C.; Moon, P.; Prince, M.; Sivakumar, S.; Tyagi, S., Jr.; Bohr, M. “

130nm Logic Technology Featuring 60nm Transistors, Low-K Dielectrics, and Cu Interconnects.” *Intel Technol. J.* **2002**, *6*, 5-13.

<http://developer.intel.com/technology/itj/2002/volume06issue02/>.

- (4) (a). *International Technology Roadmap for Semiconductors*. International SEMATECH: Austin, Tx. **1999**. ITRS documents can be accessed free of charge at <http://public.itrs.net/>.
 (b). Burggraaf, P. *Solid State Technol.* **2000**, *43*, pp. 31, 36.
- (5) (a). Lin, B. J. *J. Microlitho. Microfab. Microsys.* **2004**, *3*, 377-395. (b). Owa, S.; Nagasaka, H. *J. Microlith. Microfabr. Microsys.* **2004**, *3*, 97-103. (c). Smith, B. W.; Bourov, A.; Kang, H.; Cropanese, F.; Fan, Y.; Lafferty, N.; Zavyalova, L. *J. Microlith. Microfabr. Microsys.* **2004**, *3*, 44-51. (d). Dammel, R. R.; Houlihan, F. M.; Sakamuri, R.; Rentkiewicz, D.; Romano, A. *J. Photopolym. Sci. Technol.* **2004**, *17*, 587-602. (e). Switkes, M.; Rothschild, M. *J. Vac. Sci. Technol. B* **2001**, *19*, 2353-2356.
- (6) For reviews of the role of photoresists in lithography, see: (a) Steppan, H.; Buhr, G.; Vollman, H. *Angew. Chem. Int. Ed. Engl.* **1982**, *21*, 455-554. (b). Reichmanis, E.; Thompson, L. F. *Chem. Rev.* **1989**, *89*, 1273-1289. (c). Hinsberg, W. D.; Wallraff, G. M.; Allen, R. D. “Lithographic Resists” In *Kirk-Othmer Encyclopedia of Chemical Technology*, John Wiley & Sons. **1998**. (d). Roy, D.; Basu, P. K.; Eswaran, S. V. *Resonance* **2002**, 44-53.
- (7) Patterson, K.; Somervell, M.; Willson, C. G. *Solid State Technol.* **2000**, *43*, 41-48.
- (8) Gokan, H.; Esho, S.; Ohnishi, Y. *J. Electrochem. Soc.* **1983**, *130*, 143-146.
- (9) For reviews of the development of chemically amplified resists, see: (a). Willson, C. G.; Ito, H.; Frechet, J. M. J.; Tessier, T. G.; Houlihan, F. M. *J. Electrochem. Soc.* **1986**, *133*, 181-187. (b). Reichmanis, E.; Houlihan, F. M.; Nalamasu, O.; Neenan, T. X. *Chem. Mater.* **1991**, *3*, 394-407. (c). MacDonald, S. A.; Willson, C. G.; Frechet, J. M. *Acc. Chem. Res.* **1994**, *27*, 151-158. (d). Ito, J. *IBM J. Res. Dev.* **1997**, *41*, 69-80. (e). Stewart, M. D.;

- Patterson, K.; Somervell, M. H.; Willson, C. G. *J. Phys. Org. Chem.* **2000**, *13*, 767-774.
- (f). Ito, H. *J. Polym. Sci. A: Polym. Chem.* **2003**, *41*, 3863-3870.
- (10) (a). Reichmanis, E.; Nalamasu, O.; Houlihan, F. M. *Acc. Chem. Res.* **1999**, *32*, 659-667.
- (b). Allen, R. D.; Opitz, J.; Ito, H.; Wallow, T. I.; Casmier, D. V.; DiPietro, R. A.; Brock, P.; Breyta, G.; Sooriyakumaran, R.; Larson, C. E.; Hofer, D. C.; Varanasi, P. R.; Mewherter, A. M.; Jayaraman, S.; Vicari, R.; Rhodes, L. F.; S. Sun. *Proc. SPIE* **1999**, *3678*, 66-77.
- (11) (a). Allen, R. D.; Wallraff, G. M.; Hofer, D. C.; Kunz, R. R. *IBM J. Res. Dev.* **1997**, *41*, 95-104. (b). Allen, R. D.; Wallraff, G. M.; DiPietro, R. A.; Hofer, D. C.; Kunz, R. R. *J. Photopolym. Sci. Technol.* **1995**, *8*, 623-636. (c). Kunz, R. R.; Allen, R. D.; Hinsberg, W. D.; Walraff, G. M. *Proc. SPIE* **1993**, *1925*, 167-175.
- (12) (a). Houlihan, F. M.; Wallow, T. I.; Nalamasu, O.; Reichmanis, E. *Macromolecules* **1997**, *30*, 6517-6524. (b). Reichmanis, E.; Nalamasu, O.; Houlihan, F. M.; Wallow, T. I.; Timko, A. G.; Cirelli, R. A.; Dabbagh, G.; Hutton, R. S.; Novembre, A. E.; Smith, B. W. *J. Vac. Sci. Technol. B* **1997**, *5*, 2528-2533. (c). Nalamasu, O.; Houlihan, F. M.; Cirelli, R. A.; Timko, A. G.; Watson, G. P.; Hutton, R. S.; Gabor, A.; Medina, A.; Slater, S. *J. Vac. Sci. Technol. B* **1998**, *16*, 3716-3721. (d). Byers, J.; Patterson, K.; Cho, S.; McCallum, M.; Willson, C. G. *J. Photopolym. Sci. Technol.* **1998**, *11*, 465-474. (e). Douki, K.; Kajita, T.; Shimokawa, T. *Proc. SPIE* **2000**, *3999*, 1128-1135. (f). Park, J.-H.; Kim, J.-Y.; Seo, D.-C.; Park, S.-Y.; Lee, H.; Kim, S.-J.; Jung, J.-C.; Baik, K.-H. *Proc. SPIE* **2000**, *3999*, 1163-1170.
- (13) (a). Okoroanyanwu, U.; Shimokawa, T.; Byers, J.; Willson, C. G. *Chem. Mater.* **1998**, *10*, 3319-3327. (b). Okoroanyanwu, U.; Byers, J.; Shimokawa, T.; Willson, C. G. *Chem. Mater.* **1998**, *10*, 3328-3333. (c). Okoroanyanwu, U.; Shimokawa, T.; Byers, J.; Willson, C. G. *J. Molec. Catal. A* **1998**, *133*, 93-114. (d). Varanasi, P. R.; Jordhamo, G.; Lawson, M. C.; Chen, R.; Brunsvold, W. R.; Hughes, T.; Keller, R.; Khojasteh, M.; Li, W.; Allen, R.

- D.; Ito, H.; Opitz, J.; Truong, H.; Wallow, T. *Proc. SPIE* **2000**, 3999, 1157-1162. (e). Allen, R. D.; Opitz, J.; Wallow, T.; DiPietro, R. A.; Hofer, D. C.; Jayaraman, S.; Hullihan, K. A.; Rhodes, B. L.; Shick, R. A. *Proc. SPIE* **1998**, 3333, 463-471.
- (14) (a). Gaylord, N. G.; Mandal, B. M. *J. Polym. Sci. Polym. Lett. Ed.* **1976**, 14, 555-559. (b). Gaylord, N. G.; Desphande, A. B.; Mandal, B. M.; Marton, M.; *J. Macromol. Sci. Chem. A* **1977**, 11, 1053-1070. (c). Crivello, J. V.; Shim, S.-Y. *Chem. Mater.* **1996**, 8, 376-381.
- (15) (a). Rothschild, M.; Bloomstein, T. M.; Curtin, J. E.; Downs, D. K.; Fedynyshyn, T. H.; Hardy, D. E.; Kunz, R. R.; Liberman, V.; Sedlacek, J. H. C.; Uttaro, R. S.; Bates, A. K.; Van Peski, C. *J. Vac. Sci. Technol. B* **1999**, 17, 3262-3266. (b). Bloomstein, T. M.; Rothschild, M.; Kunz, R. R.; Hardy, D. E.; Goodman, R. B.; Palmacci, S. T. *J. Vac. Sci. Technol. B* **1998**, 16, 3154-3157. (c). Rothschild, M.; Bloomstein, T. M.; Fedynyshyn, T. H.; Liberman, V.; Mowers, W.; Sinta, R.; Switkes, M.; Grenville, A.; Orvek, K. *J. Fluor. Chem.* **2003**, 122, 3-10. (d). Wagner, C.; Kaiser, W.; Mulken, J.; Flagello, D. G. *Solid State Technol.* **2000**, 43(9), 97-108.
- (16) (a). Kunz, R. R.; Bloomstein, T. M.; Hardy, D. E.; Goodman, R. B.; Downs, D. K., Curtin, J. E. *J. Vac. Sci. Technol. B* **1999**, 17, 3267-3272. (b). Kunz, R. R.; Bloomstein, T. M.; Hardy, D. E.; Goodman, R. B.; Downs, D. K.; Curtin, J. E. *J. Photopolym. Sci. Technol.* **1999**, 12, 561-570.
- (17) (a). Fedynyshyn, T. H.; Kunz, R. R.; Doran, S. P.; Goodman, R. B.; Lind, M. L.; Curtin, J. E. *Proc. SPIE* **2000**, 3999, 335-346. (b). Cefalas, A. C.; Sarantopoulou, E.; Gogolides, E.; Argitis, P. *Microelectron. Eng.* **2000**, 53, 123-126.
- (18) Fedynyshyn, T. H.; Kunz, R. R.; Sinta, R. F.; Goodman, R. B.; Dorna, S. P. *J. Vac. Sci. Technol. B* **2000**, 18, 3332-3339.
- (19) Grandler, J. R.; Jencks, W. P. *J. Am. Chem. Soc.* **1982**, 104, 1937-1951.

- (20) Patterson, K.; Yamachika, M.; Hung, R.; Brodsky, C.; Yamada, S.; Somervell, M.; Osborn, B.; Hall, B.; Dukovic, G.; Byers, J.; Conley, W.; Willson, C. G. *Proc. SPIE*, **2000**, 3999, 365-374.
- (21) (a). Przybilla, K. J.; Roschert, H.; Pawlowski, G. *Proc. SPIE*, **1992**, 1672, 500-512. (b). Ito, H.; Seehof, N.; Sato, R. *Polym. Mater. Sci. Eng.* **1997**, 77, 449-450. (c). Ito, H.; Seehof, N.; Sato, R.; Nakayama, T.; Ueda, M. *ACS Symp. Ser.* **1998**, 706, 208-223. (d). Ito, H. *IBM. J. Res. Dev.* **2001**, 45, 683-695.
- (22) For calculations of the VUV spectra of polar, fluorinated compounds, see: (a). Matsuzawa, N. N.; Mori, S.; Yano, E.; Okazaki, S.; Ishitani, A.; Dixon, D.A. *Proc. SPIE* **2000**, 3999, 375-383. (b). Ando, S.; Fujigaya, T.; Ueda, M. *Jpn. J. Appl. Phys.* **2002**, 41, L105-L108. (c). Toriumi, M.; Satou, I.; Itani, T. *J. Vac. Sci. Technol. B* **2000**, 18, 3328-3331.
- (23) For calculations of the VUV spectra of fluorinated alkanes, see: (a). Waterland, R. L.; Dobbs, K. D.; Rinehart, A. M.; Feiring, A. E.; Wheland, R. C.; Smart, B. E. *J. Fluor. Chem.* **2003**, 122, 37-46. (b). Zhan, C. G.; Dixon, D. A.; Matsuzawa, N. N.; Ishitani, A.; Uda, T. *J. Fluor. Chem.* **2003**, 122, 27-35.
- (24) (a). Brodsky, C.; Byers, J.; Conley, W.; Hung, R.; Yamada, S.; Patterson, K.; Somervell, M.; Trinqué, B.; Tran, H. V.; Cho, S.; Chiba, T.; Lin, S. H.; Jamieson, A.; Johnson, H.; Vander Heyden, T.; Willson, C. G. *J. Vac. Sci. Technol. B* **2000**, 18, 3396-3401. (b). Chiba, T.; Hung, R. J.; Yamada, S.; Trinqué, B.; Yamachika, M. Brodsky, C.; Patterson, K.; Vander Heyden, A.; Jamison, A.; Lin, S. H.; Somervell, M.; Byers, J.; Conley, W.; Willson, C.G. *J. Photopolymer Sci. Technol.* **2000**, 13, 657-664.
- (25) (a). Ito, H.; Miller, D. C.; Willson, C. G. *Macromolecules* **1982**, 15, 915-920. (b). Wilson, C. G.; Ito, H.; Miller, D. C.; Tessier, T. G. *Polym. Eng. Sci.* **1983**, 23, 1000-1003.
- (26) (a). French, R. H.; Wheland, R. C.; Jones, D. J.; Hilfiker, J. N.; Synowicki, R. A.; Zumsteg, F. C.; Fledman, J.; Feiring, A. E. *Proc. SPIE* **2000**, 4000, 1491-1502. (b). Johs, B.; French, R. C.; Kalk, F. D.; McGahan, W. A.; Woollam, J. A. *Proc. SPIE* **1994**, 2253, 1098-1106.

- (27) (a). Ito, H.; Wallraff, G. M.; Brock, P.; Fender, N.; Truong, H.; Breyta, G.; Miller, D. C.; Sherwood, M. H.; Allen, R. D. *Proc. SPIE* **2001**, *4345*, 273-284. (b). Trinque, B. C.; Chiba, T.; Hung, R. J.; Chambers, C. R.; Pinnow, M. J.; Osborn, B. P.; Tran, H. V.; Wunderlich, J.; Hsieh, Y.-T.; Thomas, B. H.; Shafer, G.; DesMarteau, D. D.; Conley, W.; Willson, C. G. *J. Vac. Sci. Technol. B* **2002**, *20*, 531-536. (c). Ito, H.; Okazaki, M.; Miller, D. C. *J. Polym. Sci. A: Polym. Chem.* **2004**, *42*, 1468-1477.
- (28) Schmaljohann, D.; Bae, Y. C.; Weibel, G. L.; Hamad, A. H.; Ober, C. K. *Proc. SPIE* **2000**, *3999*, 330-334. (b). Schmaljohann, D.; Bae, Y. C.; Dai, J.; Weibel, G. L.; Hamad, A.; Ober, C. K. *J. Photopolym. Sci. Technol.* **2000**, *13*, 451-458.
- (29) (a). Tran, H. V.; Hung, R. J.; Chiba, T.; Yamada, S.; Mrozek, T.; Hsieh, Y.-T.; Chambers, C. R.; Osborn, B. P.; Trinque, B. C.; Pinnow, M. J.; Sanders, D. P.; Connor, E. F.; Grubbs, R. H.; Conley, W.; MacDonald, S. A.; Willson, C. G. *J. Photopolym. Sci. Technol.* **2001**, *14*, 669-674. (b). Hung, R.; Tran, H. V.; Trinque, B. Chiba, T.; Yamada, S.; Osborn, B.; Brodsky, C.; Vander Heyden, A.; Sanders, D.; Grubbs, R.; Klopp, J.; Frechet, J.; Thomas, B.; Shafer, G.; , D.; Conley, W.; Willson, C. G. *Proc. SPIE.* **2001**, *4345*, 385-395. (c). Willson, C. G.; Trinque, B. C.; Osborn, B. P.; Chambers, C. R.; Hsieh, Y.-T.; Chiba, T.; Zimmerman, P.; Miller, D.; Conley, W. *J. Photopolym. Sci. Technol.* **2002**, *15*, 583-590. (d). Hoskins, T.; Chung, W. J.; Agrawal, A.; Ludovice, P. J.; Henderson, C. L.; Seger, L. D.; Rhodes, L. F.; Shick, R. A. *Macromolecules* **2004**, *37*, 4512-4518.
- (30) (a). Kodama, S.; Kaneko, I.; Takebe, Y.; Okada, S.; Kawaguchi, Y.; Shida, N.; Ishikawa, S.; Toriumi, M.; Itani, T. *Proc. SPIE* **2002**, *4690*, 76-83. (b). Toriumi, M.; Shida, N.; Watanabe, H.; Yamazaki, T.; Ishikawa, S.; Itani, T. *Proc. SPIE* **2002**, *4690*, 191-199. (c). Shida, N.; Watanabe, H.; Yamazaki, T.; Ishikawa, S.; Toriumi, M.; Itani, T. *Proc. SPIE* **2002**, *4690*, 497-503.
- (31) (a). Crawford, M. K.; Feiring, A. E.; Fledman, J.; French, R. H.; Periyasamy, M.; Schadt, F. L., III.; Smalley, R. J.; Zumsteg, F. C.; Kunz, R. R.; Rao, V.; Liao, L.; Holl, S. M. *Proc.*

- SPIE* **2000**, 3999, 357-364. (b). French, R. C.; Feldman, J.; Zumsteg, F. C.; Crawford, M. K.; Feiring, A. E.; Petrov, V. A.; Schadt, F. L., III.; Wheland, R. C.; Gordon, J.; Zhang, E. *Semicond. FABTECH* **2001**, 14, 167-175. (c). Feiring, A. E.; Crawford, M. K.; Farnham, W. B.; Feldman, J.; French, R. H.; Leffew, K. W.; Petrov, V. A.; Schadt, F. L., III.; Wheland, R. C.; Zumsteg, F. C. *J. Fluor. Chem.* **2003**, 122, 11-16. (d). Toriumi, M.; Ishikawa, T.; Kodani, T.; Koh, M.; Moriya, T.; Araki, T.; Aoyama, H.; Yamashita, T.; Yamazaki, T.; Furukawa, T.; Itani, T. *J. Photopolym. Sci. Technol.* **2003**, 16, 607-614. (e). Toriumi, M.; Ishikawa, T.; Kodani, T.; Koh, M.; Moriya, T.; Yamashita, T.; Araki, T.; Aoyama, H.; Yamazaki, T.; Furukawa, T.; Itani, T. *J. Vac. Sci. Technol. B* **2004**, 22, 27-30.
- (32) (a). Barnes, D. A.; Benedikt, G. M.; Goodall, B. L.; Huang, S. S.; Kalamarides, H. A.; Lenhard, S.; McIntosh, L. H., III.; Selvy, K. T.; Shick, R. A.; Rhodes, L. F. *Macromolecules* **2003**, 36, 2623-2632. (b). Park, K. H.; Twieg, R. J.; Ravikiran, R.; Rhodes, L. F.; Shick, R. A.; Yankelevich, D.; Knoesen, A. *Macromolecules* **2004**, 37, 5163-5178. (c). Lin, S. T.; Narske, R. N.; Klabunde, K. J. *Organometallics* **1985**, 4, 571-574.
- (33) (a). Sen, A.; Lai, T.-L. *Organometallics* **1982**, 1, 415-417. (b) Sen, A.; Lai, T-W; Thomas, R. R. *J. Organomet. Chem.* **1988**, 358, 567-588. (c) Mehler, C.; Risse, W. *Makromol. Chem. Rapid. Commun.* **1991**, 12, 255-259. (d). Mehler, C.; Risse, W. *Macromolecules* **1992**, 12, 4226-4228. (e). Seehof, N.; Mehler, C.; Breunig, S.; Risse, W. *J. Molec. Catal.* **1992**, 76, 219-228. (f). Lipian, J.; Mimna, R. A.; Fondran, J. C.; Yandulov, D.; Shick, R. A.; Goodall, B. L.; Rhodes, L. F.; Huffman, J. C. *Macromolecules* **2002**, 35, 8969-8977.
- (34) (a). Breunig, S.; Risse, W. *Makromol. Chem.* **1992**, 193, 2915-2927. (b). Mehler, C.; Risse, W. *Makromol. Chem., Rapid Commun.* **1992**, 13, 455-459. (c). Reinmuth, A.; Mathew, J. P.; Melia, J.; Risse, W. *Macromol. Rapid Commun.* **1996**, 17, 173-180. (d). Mathew, J. P.; Reinmuth, A.; Melia, J.; Swords, N.; Risse, W. *Macromolecules* **1996**, 39, 2755-2763.

- (35) (a). Hennis, A. D.; Polley, J. D.; Long, G. S.; Sen, A.; Yandulov, D.; Lipian, J.; Benedikt, G. M.; Rhodes, L. F.; Huffman, J. *Organometallics* **2001**, *20*, 2802-2812. (b). Goodall, B. L.; Barnes, D. A.; Benedikt, G. M.; McIntosh, L. H.; Rhodes, L. F. *Polym. Mat. Sci. Eng.* **1997**, *76*, 56-57.
- (36) Peruch, F.; Risse, W. *Polym. Prepr.* **2000**, *41*, 1916-1917.
- (37) (a). Kang, M.; Sen, A. *Organometallics* **2004**, *23*, 5396-5398. (b). Funk, J. K.; Andes, C. E.; Sen, A. *Organometallics* **2004**, *23*, 1680-1683. (c). Funk, J. K.; Andes, C.; Sen, A. *Polym. Prepr.* **2003**, *44*, 681-682. (d). Hennis, A. D.; Sen, A. *Polym. Prepr.* **2000**, *41*, 1933-1934.
- (38) (a). Martin, J. G.; Hill, R. K. *Chem. Rev.* **1961**, *16*, 537-562. (b). Madan, R.; Srivastava, A.; Anand, R. C.; Varma, I. K. *Prog. Polym. Sci.* **1998**, *23*, 621-663.
- (39) Heinz, B. S.; Alt, F. P.; Heitz, W. *Macromol. Rapid. Commun.* **1998**, *19*, 251-256.
- (40) (a). Michalak, A.; Ziegler, T. *Organometallics* **2004**, *23*, 5565-5572. (b). Michalak, A.; Ziegler, T. *Organometallics* **2001**, *20*, 1521-1532.
- (41) (a). Trinque, B. C.; Chambers, C. R.; Osborn, B. P.; Callahan, R. P.; Lee, G. S. Kusumoto, S.; Sanders, D. P.; Grubbs, R. H.; Conley, W. E.; Willson, C. G. *J. Fluor. Chem.* **2003**, *122*, 17-26. (b). Trinque, B. C.; Osborn, B. P.; Chambers, C. R.; Hsieh, Y.-T.; Corry, S.; Chiba, T.; Hung, R. J.; Tran, H. V.; Zimmerman, P.; Miller, D.; Conley, W.; Wilson, C. G. *Proc. SPIE* **2002**, *4690*, 58-68.
- (42) Osborn, B. P.; Chiba, T.; Trinque, B. C.; Brodsky, C. J.; Hung, R. J.; Tran, H. V.; Chambers, C. R.; Callahan, R. P.; Carpenter, II., L. E.; Pinnow, M. J.; Lee, G. S.; Yamachika, M.; Willson, C. G.; Sanders, D. P.; Grubbs, R. H.; Dixon, D. A.; Miller, D. A.; Conley, W. E. Manuscript in preparation. For more calculations of the VUV spectra of fluorinated norbornenes, see: (a). Dixon, D. A.; Matsuzawa, N. N.; Ishitani, A.; Uda, T. *Phys. Stat. Sol B* **2001**, *226*, 69-77. (b). Matsuzawa, N. N.; Ishitani, A.; Dixon, D. A.; Uda,

- T. *Proc. SPIE* **2001**, 4345, 396-405. (c). Yamazaki, T.; Itani, T. *Jpn. J. Appl. Phys.* **2003**, 42, 3881-3884.
- (43) Exposure of bicyclo[2.2.2]oct-2-ene to a (π -allyl) palladium hexafluoroantimonate catalyst results in no polymer formation.
- (44) Huisgen, R. Ooms, P. H. J.; Mingin, M.; Allinger, N. A. *J. Am. Chem. Soc.* **1980**, 102, 3951-3953.
- (45) Atkinson, R.; Aschmann, S. M.; Carter, W. P. L.; Pitts, J. N., Jr. *Int. J. Chem. Kinetics* **1983**, 15, 721-731.
- (46) Osborn, B. P. *Ph.D. Dissertation* University of Texas-Austin, **2004**.
- (47) (a). Grubbs, R. H.; Trnka, T. M.; Sanford, M. S. *Curr. Meth. Inorg. Chem.* **2003**, 187- 231.
(b). Grubbs, R. H. *Tetrahedron* **2004**, 60, 7117-7140.
- (48) For recent reviews on olefin cross-metathesis, see: (a). Chatterjee, A. K. In *Handbook of Olefin Metathesis*, vol. 2., Grubbs, R. H., Ed. Wiley-VCH: Weinheim, Ge., **2004**, pp. 246-295. (b). Connon, S. J.; Blechert, S. *Angew. Chem. Int. Ed.* **2003**, 42, 1900-1923.
- (49) For reviews on ring-closing metathesis, see: (a). Maier, M. E. *Angew. Chem. Int. Ed.* **2000**, 39, 2073-2077. (b). Grubbs, R. H.; Miller, S. J.; Fu, G. C. *Acc. Chem. Rec.* **1995**, 28, 446-452.
- (50) For a recent review on ADMET, see: Schwendeman, J. E.; Church, A. C.; Wagener, K. B. *Adv. Synth. Catal.* **2002**, 344, 597-613.
- (51) For recent reviews on development of olefin metathesis catalysts and their application to ring-opening metathesis polymerization, see: (a). Buchmeiser, M. R. *Chem. Rev.* **2000**, 100, 1565-1604. (b) Frenzel, U.; Nuyken, O. *J. Polym. Sci. A Polym. Chem.* **2002**, 40, 2895-2916. (c). Slugovc, C. *Macromol. Rapid Commun.* **2004**, 25, 1283-1297. (d). Trnka, T. M.; Grubbs, R. H. *Acc. Chem. Res.* **2001**, 34, 18-29.
- (52) Ivin, K. J. *Makromol. Chem. Macromo., Symp.* **1991**, 42/43, 1-14.

- (53) For recent reviews on development of olefin metathesis catalysts, see: (a) Schrock, R. R. In *Handbook of Olefin Metathesis*, vol. 1., Grubbs, R. H., Ed. Wiley-VCH: Weinheim, Ge., **2004**, pp. 8-32. (b) Nguyen, S. T.; Trnka, T. M. In *Handbook of Olefin Metathesis*, vol. 1., Grubbs, R. H., Ed. Wiley-VCH: Weinheim, Ge., **2004**, pp. 61-85. (c) Trnka, T. M.; Grubbs, R. H. *Acc. Chem. Res.* **2001**, *34*, 18-29.
- (54) (a) Schrock, R. R.; Murdzek, J. S.; Bazan, G. C.; Robbins, J.; Dimare, M.; O'Regan, M. J. *Am. Chem. Soc.* **1990**, *112*, 3875-3886. (b) Bazan, G. C.; Khosravi, E.; Schrock, R. R.; Feast, W. J.; Gibson, V. C.; O'Regan, M. B.; Thomas, J. K.; Davis, W. M. *J. Am. Chem. Soc.* **1990**, *112*, 8378-8387. (c) Bazan, G. C.; Oskam, J. H.; Cho, H. N.; Park, L. Y.; Schrock, R. R. *J. Am. Chem. Soc.* **1991**, *113*, 6899-6907.
- (55) (a) Schwab, P.; France, M. B.; Ziller, J. W.; Grubbs, R. H. *Angew. Chem. Int. Ed. Eng.* **1995**, *34*, 2039-2041. (b) Schwab, P.; Grubbs, R. H.; Ziller, J. W. *J. Am. Chem. Soc.* **1996**, *118*, 100-110. (c) Belderrain, T. R.; Grubbs, R. H. *Organometallics* **1997**, *16*, 4001-4003.
- (56) (a) Scholl, M.; Ding, S.; Lee, C. W.; Grubbs, R. H. *Org. Lett.* **1999**, *1*, 953-956. (b) Sanford, M. S.; Love, J. A.; Grubbs, R. H. *J. Am. Chem. Soc.* **2001**, *123*, 6543-6554.
- (57) For a recent review, see: (a) Hoveyda, A. H.; Gillingham, D. G.; Van, Velhuizen, J. J.; Kataoka, O.; Garber, S. B.; Kingsbury, J. S.; Harrity, J. P. A. *Org. Biomol. Chem.* **2004**, *2*, 8-23. Also: (b) Kingsbury, J. S.; Harrity, J. P. A.; Bonitatebus, P. J.; Hoveyda, A. H. *J. Am. Chem. Soc.* **1999**, *121*, 791-799. (c) Garber, S. B.; Kingsbury, J. S.; Gray, B. L.; Hoveyda, A. *J. Am. Chem. Soc.* **2000**, *122*, 8168-8179.
- (58) (a) Sanford, M. S.; Love, J. A.; Grubbs, R. H. *Organometallics* **2001**, *20*, 5314-5318. (b) Love, J. A.; Morgan, J. P.; Trnka, T. M.; Grubbs, R. H. *Angew. Chem. Int. Ed.* **2002**, *41*, 4035-4037.
- (59) (a) Slugovc, C.; Demel, S.; Stelzer, F. *Chem. Commun.* **2002**, 2572-3. (b) Choi, T.-L.; Grubbs, R. H. *Angew. Chem. Int. Ed.* **2003**, *42*, 1743-1746. (c) Slogovc, C.; Riegler, S.; Hayn, G.; Saf, R.; Stelzer, F. *Macromol. Rapid. Commun.* **2003**, *24*, 435-439.

- (60) Bielawski, C. W.; Benitez, D.; Morita, T.; Grubbs, R. H. *Macromolecules* **2001**, *34*, 8610-8618.
- (61) (a). Yoshida, Y.; Goto, K.; Komiya, Z. *J. Appl. Polym. Sci.* **1997**, *66*, 367-375. (b). Otsuki, T.; Goto, K.; Komiya, Z. *J. Polym. Sci. A: Polym. Chem.* **2000**, *66*, 367-375.
- (62) Hatjopoulos, J. D.; Register, R. A. *Polym. Mat. Sci. Eng.* **2004**, *91*, 971-972.
- (63) (a). Mol, J. C. *J. Molec. Catal. A: Chem.* **2004**, *213*, 39-45. (b). Yamazaki, M. *J. Molec. Catal. A: Chem.* **2004**, *213*, 81-87. (c). Six, C.; Beck, K.; Wegner, A.; Leitner, W. *Organometallics* **2000**, *19*, 4639-4642.
- (64) Preishuber-Pfugl, P.; Eder, E.; Stelzer, F.; Reisinger, H.; Mulaupf, R.; Forsyth, J.; Perena, J. M. *Macromol. Chem. Phys.* **2001**, *202*, 1130-1137.
- (65) Contrearras, A. P.; Cerda, A. M.; Tlenkopatchev, M. A. *Macromol. Chem. Phys.* **2002**, *203*, 1811-1818.
- (66) (a). Feast, W. J.; Gimeno, M.; Khosravi, E. *Polymer* **2003**, *44*, 6111-6121. (b). Feast, W. J.; Gimeno, M.; Khosravi, E. *J. Molec. Catal. A: Chem.* **2004**, *44*, 9-14. (c). Feast, W. J.; Gimeno, M.; Khosravi, E. *J. Fluor. Chem.* **1999**, *100*, 117-125. (d). Yampol'skii, Y. P.; Bepalova, N. B.; Finkelshtein, E. S.; Bondar, V. I.; Popov, A. V. *Macromolecules* **1994**, *27*, 2872-2878. (e). Seehof, N.; Grutke, S.; Risse, W. *Macromolecules* **1993**, *26*, 695-700.
- (67) Patterson, K. W. *Ph.D. Dissertation* University of Texas, Austin, **2000**.